



ISTITUTO NAZIONALE DI RICERCA METROLOGICA Repository Istituzionale

Report on EURAMET supplementary comparison on measurement of a 1 mm stage micrometer

Original

Report on EURAMET supplementary comparison on measurement of a 1 mm stage micrometer / Matus, M; Pérez, M del Mar; Prieto, E; Germak, A; Czulek, D; Sosinowski, P; Duță, A; Dugheanu, E; Zelenika, S; Äremann, M; Ozgur, B; Asar, M; Greeff, P; Manana, K; Sun, S; Buajarern, J; Brasil, D A; Gastaldi, B; Zechner, G. - In: METROLOGIA. - ISSN 0026-1394. - 61:1A(2024). [10.1088/0026-1394/61/1a/04003]

Availability:

This version is available at: 11696/83579 since: 2025-01-24T16:34:07Z

Publisher:

IOP

Published

DOI:10.1088/0026-1394/61/1a/04003

Terms of use:

This article is made available under terms and conditions as specified in the corresponding bibliographic description in the repository

Publisher copyright

BIPM
Copyright © BIPM. The BIPM holds copyright on the textual and multimedia information available on BIPM website, which includes titles, slogans, logos and images, unless otherwise stated. All commercial use, reproduction or translation of textual and multimedia information and/or of the logos, emblems, publications or other creations contained therein, requires the prior written permission of the BIPM.

(Article begins on next page)

**Report on EURAMET Supplementary Comparison
Measurement of a 1 mm Stage Micrometer
EURAMET project 1488
EURAMET.L-S2.3.n02
(previously EURAMET.L-S29)**

M Matus (BEV),

E Prieto (CEM), M Pérez (CEM), A Germak (INRIM), D Czulek (GUM), P Sosinowski (GUM),
A Duță (INM), E Dugheanu (INM), S Zelenika (DMDM), M Äremann (RISE),
B Ozgur (UME), M Asar (UME), P Greeff (NMISA), K Manana (NMISA), S Sun (NIM),
J Buajareern (NIMT), D A Brasil (INMETRO), B Gastaldi (NMI)

Wien, June 2024

Contents

| | | |
|-------|---|----|
| 1 | Document control..... | 4 |
| 2 | Introduction | 4 |
| 3 | Organization..... | 4 |
| 3.1 | Participants..... | 4 |
| 3.2 | Schedule | 5 |
| 4 | Artefacts..... | 6 |
| 4.1 | Description of artefacts | 6 |
| 4.2 | Stability of artefacts | 7 |
| 4.3 | Condition of artefacts at start/end of comparison | 8 |
| 4.3.1 | Artefact 1 | 8 |
| 4.3.2 | Artefact 2 | 10 |
| 5 | Measuring instructions | 11 |
| 5.1 | Handling the artefact | 11 |
| 5.2 | Cleaning..... | 12 |
| 5.3 | Traceability | 12 |
| 5.4 | Measurands | 12 |
| 5.5 | Measurement uncertainty..... | 13 |
| 5.6 | Reference condition | 13 |
| 6 | Results..... | 13 |
| 6.1 | Results and standard uncertainties as reported by participants..... | 13 |
| 6.2 | Measurement uncertainties | 17 |
| 6.3 | Changes to results after Draft A.1..... | 18 |
| 6.4 | Calculation of the SCR.V | 18 |
| 6.5 | Calculation of Degrees of Equivalence | 20 |
| 6.5.1 | Tabular representation of DoE results | 21 |
| 6.5.2 | Graphical representation of DoE results for selected line marks | 22 |
| 6.5.3 | Tabular representation of normalized DoE results (E_n)..... | 28 |
| 6.6 | Discussion of results..... | 29 |
| 6.6.1 | Reported and published measurement uncertainties | 30 |
| 6.7 | Linking of result to other comparisons | 31 |
| 7 | Equipment and measuring processes of the participants..... | 31 |
| 7.1 | BEV | 32 |
| 7.2 | GUM | 33 |
| 7.3 | INM..... | 34 |

| | | |
|------|---------------|----|
| 7.4 | DMDM | 35 |
| 7.5 | NIM..... | 36 |
| 7.6 | NIMT..... | 37 |
| 7.7 | INMETRO | 38 |
| 7.8 | INTI | 40 |
| 7.9 | CEM | 41 |
| 7.10 | INRIM..... | 43 |
| 7.11 | RISE..... | 45 |
| 7.12 | UME..... | 47 |
| 7.13 | NMISA..... | 48 |

1 Document control

| | |
|-------------------|----------------------------|
| Version Draft A.1 | Issued on 21. October 2022 |
| Version Draft B.0 | Issued on 19. March 2024 |
| Version Draft B | Issued on 23. April 2024 |
| Final Version | Issued on 17. June 2024 |

2 Introduction

The metrological equivalence of national measurement standards and of calibration certificates issued by national metrology institutes is established by a set of key and supplementary comparisons chosen and organized by the Consultative Committees of the CIPM or by the regional metrology organizations in collaboration with the Consultative Committees.

At its meeting in Espoo, 16-17 October 2017, the EURAMET Technical Committee for Length (TC-L) decided to carry out a supplementary comparison on stage micrometer measurements, named EURAMET.L-S29, with BEV (Bundesamt für Eich- und Vermessungswesen) as the pilot laboratory. The results of this international comparison will support the Calibration and Measurement Capabilities (CMCs) declared by the NMIs in the CIPM Mutual Recognition Arrangement (MRA). The comparison was registered in November 2019 at EURAMET and January 2020 at KCDB. Artefact circulation started in August 2020 and was completed in September 2022.

3 Organization

3.1 Participants

Table 1. List of participant laboratories and their contacts.

| Laboratory, Country code RMO | Contact person, Laboratory | Phone Email |
|------------------------------------|---|---|
| BEV (AT) EURAMET Pilot | Michael Matus Bundesamt für Eich- und Vermessungswesen Arltgasse 35, A-1160 Wien, Austria | +43 1 21110 826540 michael.matus@bev.gv.at |
| CEM (ES) EURAMET | Emilio Prieto ^{*)} , M ^a Mar Pérez Centro Español de Metrología Alfar 2, ES-28760 Tres Cantos (Madrid), Spain | +34 91 8074 716 / 801 eprieto@cem.es mmperezh@cem.es |
| INRIM (IT) EURAMET | Alessandro Germak Istituto Nazionale di Ricerca Metrologica Strada delle Cacce 91, 10135 Torino, Italy | +39 011 3919 924 a.germak@inrim.it |
| GUM (PL) EURAMET | Dariusz Czulek, Piotr Sosinowski Central Office of Measures ul. Elektoralna 2, 00-139 Warszawa, Poland | +48 22 581 95 43/07 dariusz.czulek@gum.gov.pl piotr.sosinowski@gum.gov.pl |
| INM (RO) EURAMET | Alexandru Duță ^{*)} , Elena Dugheanu National Institute of Metrology Sos. Vitan-Bârzesti 11, 042122 Bucuresti, Romania | +40 21 334 5060 alexandru.duta@inm.ro elena.dugheanu@inm.ro |
| DMDM (RS) EURAMET | Slobodan Zelenika Directorate of Measures and Precious Metals Mike Alasa 14, YU - 11 000 Belgrad, Serbia | +381 11 20 24 421 zelenika@dmdm.rs |
| RISE (SE) EURAMET | Marianne Äremann RISE Research Institutes of Sweden AB 50115 Borås, Sweden | +46 10 516 5492 or 5481 +46 70 280 54 92 marianne.aremenn@ri.se |

| | | |
|------------------------|---|--|
| UME (TR) EURAMET | Bulent Ozgur, Muharrem Asar Ulusal Metroloji Enstitüsü Barış Mah. Dr. Zeki Acar Cad. No:1 41470 Gebze, Kocaeli, Türkiye | +90 262 679 50 00 ext. 5300 bulent.ozgur@tubitak.gov.tr muharrem.asar@tubitak.gov.tr |
| NMISA (ZA) AFRIMETS | Pieter Greeff ^{*)} , Kenneth Manana National Metrology Institute of South Africa Building 5 CSIR Campus, Brummeria, Pretoria 0184, South Africa | +27 12 841 4936 pgreeff@nmisa.org kmanana@nmisa.org |
| NIM (CN) APMP | Shuanghua Sun National Institute of Metrology No. 18, Bei San Huan Dong Rd. 100029 Beijing, China | +86 10 64524911 sunshh@nim.ac.cn |
| NIMT (TH) APMP | Jariya Buajarern National Institute of Metrology Thailand 3/4-5 Moo 3, Klong 5, Klong Luan 12120 Pathumthani, Thailand | +66 2 5775100 1216 jariya@nimt.or.th |
| INMETRO (BR) SIM | Davi Anders Brasil INMETRO Av. N. S. das Graças, 50 – Vila Operária - Xerém Duque de Caxias – RJ, Brazil | +55 21 2145 3289 dabrasil@inmetro.gov.br |
| INTI (AR) SIM | Bruno Gastaldi Instituto Nacional de Tecnología Industrial Av. Vélez Sarsfield 1561, Córdoba X5000JKC, Argentina | +54 0351 4684835 gastaldi@inti.gob.ar |

*) Contacts retired or are on leave in the course of the project.

3.2 Schedule

The comparison was carried out in the form of a circulation. After the first three participants the original artefact suffered from a massive contamination and deterioration of the scale marks. Finally, a new artefact had to be acquired and characterized. This caused a significant delay in the circulation as shown in Table 2. It was decided to withdraw the results from participant starting from CEM on who first reported the contamination. CEM, RISE and INRIM were scheduled to calibrate the second artefact (Table 2) in loop 2.

Table 2. Schedule of the comparison. First artefact (loop 1)

| RMO | Laboratory | Original schedule | Date of measurement | Results received |
|-----------|------------|-------------------|---------------------|------------------|
| EURAMET | BEV | August 2020 | August 2020 | August 2020 |
| EURAMET | GUM | September 2020 | September 2020 | December 2020 |
| EURAMET | INM | October 2020 | October 2020 | November 2020 |
| EURAMET | CEM | November 2020 | November 2020 | — (discarded) |
| EURAMET | RISE | December 2020 | December 2020 | — (discarded) |
| EURAMET | INRIM | January 2021 | — | — |
| Pilot Lab | BEV | — | January 2021 | — |

Table 3 Schedule of the comparison. Second artefact (loop 2)

| RMO | Laboratory | Original schedule | Date of measurement | Results received |
|---------|------------|-------------------|---------------------|------------------|
| EURAMET | BEV | — | February 2021 | February 2021 |
| EURAMET | DMDM | | March 2021 | May 2021 |
| APMP | NIM | | April 2021 | June 2021 |
| APMP | NIMT | | June 2021 | August 2021 |

| | | | | |
|-----------|---------|---|----------------|---------------|
| SIM | INMETRO | | July 2021 | October 2021 |
| SIM | INTI | | August 2021 | November 2021 |
| Pilot Lab | BEV | — | January 2022 | — |
| EURAMET | CEM | | February 2022 | May 2022 |
| EURAMET | INRIM | | March 2022 | June 2022 |
| EURAMET | RISE | | April 2022 | May 2022 |
| Pilot Lab | BEV | — | May 2022 | — |
| EURAMET | UME | | June 2022 | November 2022 |
| AFRIMETS | NMISA | | September 2022 | November 2022 |
| Pilot Lab | BEV | — | September 2022 | — |

For both loops BEV contributed with the respective first measurement only.

4 Artefacts

4.1 Description of artefacts

Both artefacts are typical stage micrometers with fairly well-defined graduation lines (Figure 1). Both are of equal type and of the same manufacturer. The scale length is 1 mm divided in 100 parts. The graduation lines have a width of approximately 3 μm and are of unequal length. 11 lines are numerical labelled in multiples of 0.1 mm (Figure 2). No cover glass is applied to the scale.

Substrate dimensions: 75.7 mm \times 25.8 mm \times 2.2 mm

Substrate material: Nextrema[®] 724-3¹

Linear thermal expansion coefficient: $(-0.1 \pm 0.7) \cdot 10^{-6} \text{ K}^{-1}$

Lines: vacuum deposited chromium



Figure 1 Stage micrometer

¹ Information by manufacturer <https://www.schott.com/nextrema>

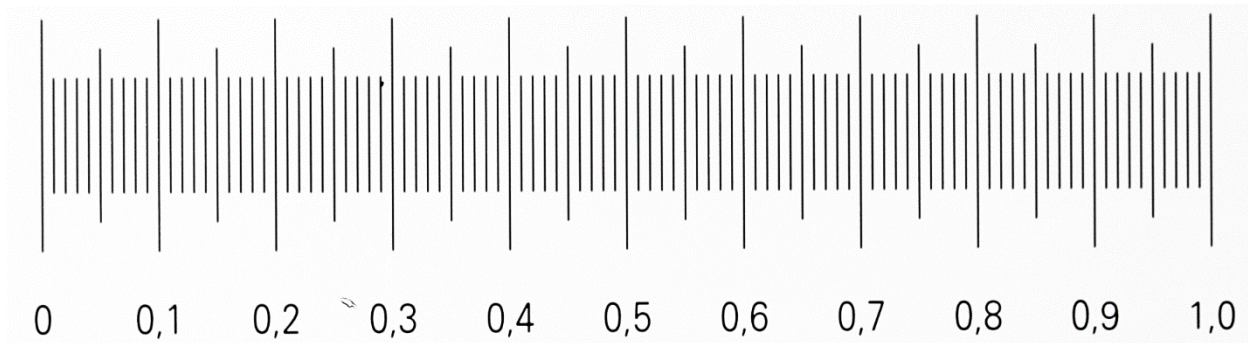


Figure 2 Microphotography of the scale

Figure 3 shows the special plastic case designed for the artefact. When properly closed with the yellow clip, the stage micrometer is securely fixed between two rubber membranes. Both membranes have a circular hole in the center. The stage micrometer can be placed in a way so that the scale is not touched by the membranes or by any other object.

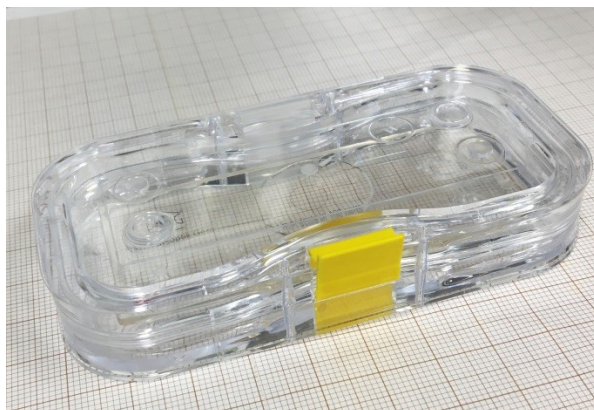


Figure 3 Transporting case. Properly closed



Figure 4 Transporting case. Placement of the artefact

4.2 Stability of artefacts

A total of four stability measurements during the course of the comparison were scheduled by the pilot laboratory. However, the original artefact was damaged after the first three participants. Only the stability of the second artefact could thus be characterized. Since both artefacts are of same make and kind, it is very likely that both are of similar stability.

Artefact 2 was measured by the pilot at the start and at the end of the circulation. Additionally, two more measurements could be performed in between (Figure 5). The total time span was 19 months. The maximum total span over all measurements and all 100 distances was 8 nm (Figure 6). This is considerable smaller than the pilot's standard uncertainty of 24 nm. The artefact can be regarded as stable within the 95 % confidence level; hence no uncertainty has to be added to the SCR.V.

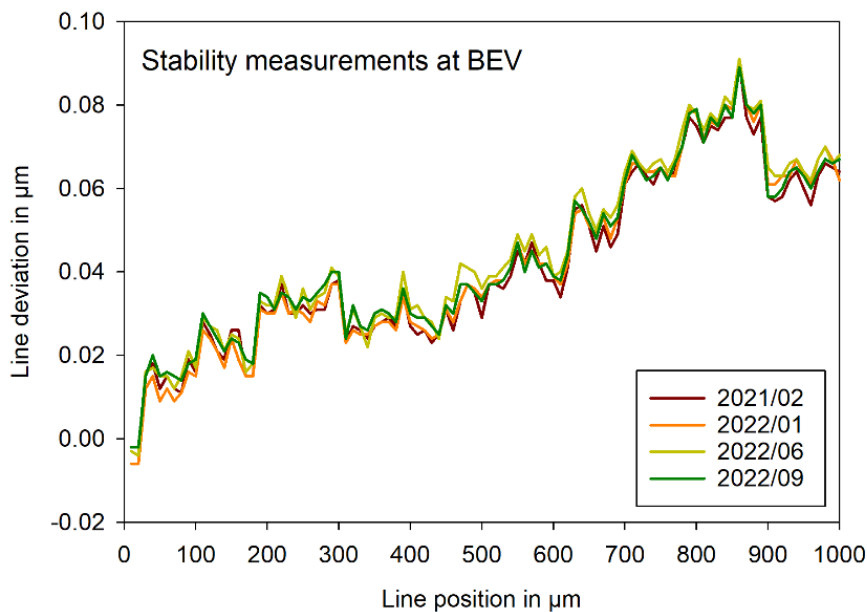


Figure 5 Stability of artefact 2 used in loop 2. Four measurements of the pilot laboratory superimposed. The standard uncertainty of each measurement is $0.024 \mu\text{m}$.

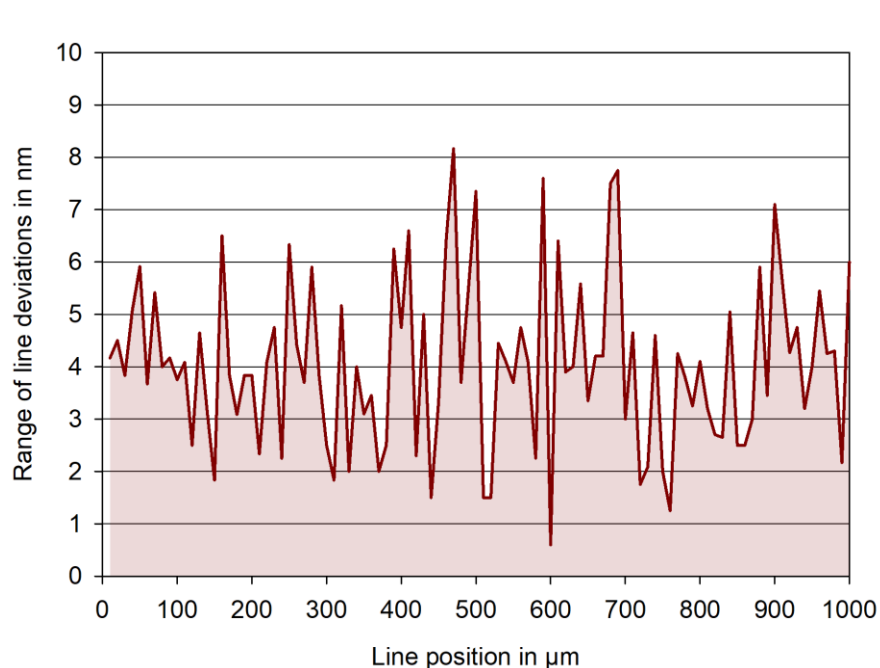


Figure 6 Stability of artefact 2 used in loop 2. Total range of the four measurements plotted in Figure 5 for each individual line.

4.3 Condition of artefacts at start/end of comparison

4.3.1 Artefact 1

As described earlier, artefact 1 (used for loop 1) was massively contaminated after three participants. CEM was the first participant who documented the bad condition of the artefact. After return to the pilot

not only a contamination but a deformation of the chromium pattern was noticed. This is already visible in Figure 7, taken prior to any cleaning attempts.

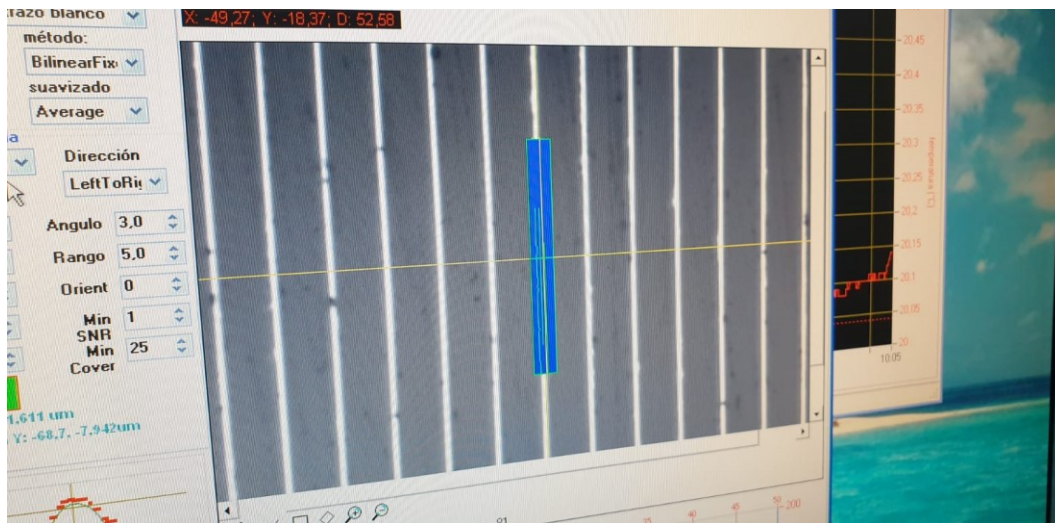


Figure 7 Image of artefact 1 in the measurement system of CEM. Picture taken before the cleaning process in November 2020.

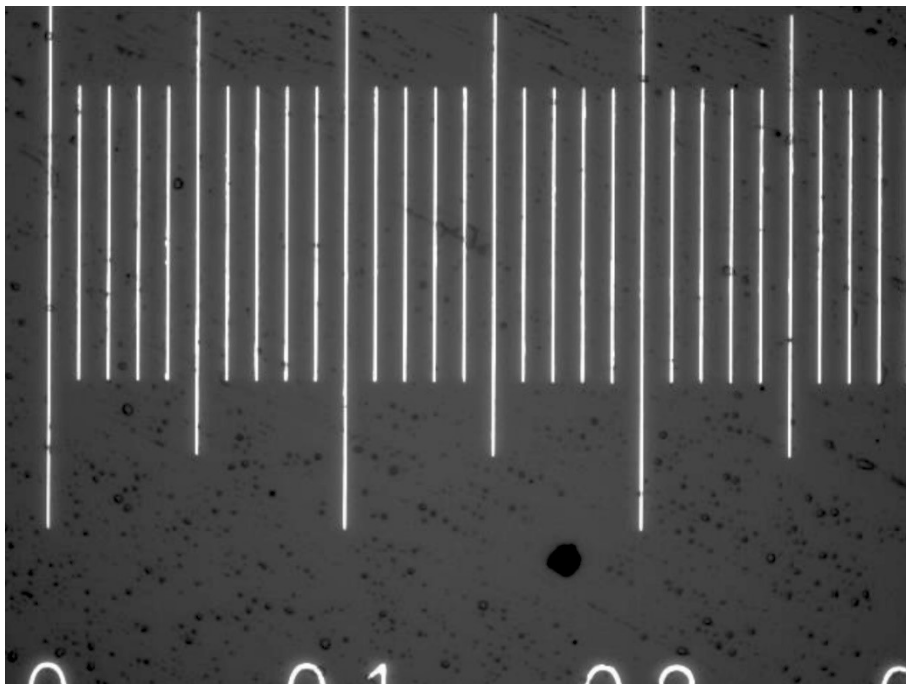


Figure 8 Microphotograph of artefact 1 taken by RISE in December 2020.

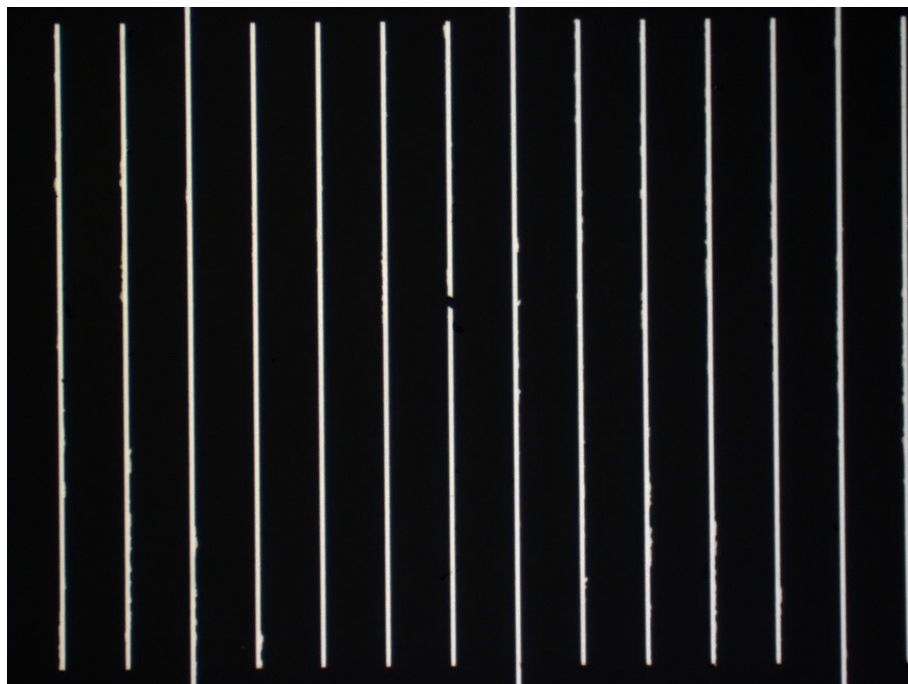


Figure 9 Artefact 1. Line at 360 μm with a gap in the region to be measured. Other lines show asymmetric chromium spreading. This influences the line center position significantly. Microphotograph taken by BEV after return of the sample in January 2021.

4.3.2 Artefact 2

For artefact 2 used for loop 2 the microscopic investigation does not show any significant change of the condition. Some dust particles accumulated during the circulation, most of them outside the measurement area.

In June 2021 NIM was the first participant who has sent reports of these contaminations as shown in Figure 10. It was possible to blow away the particles by clean and dry air.

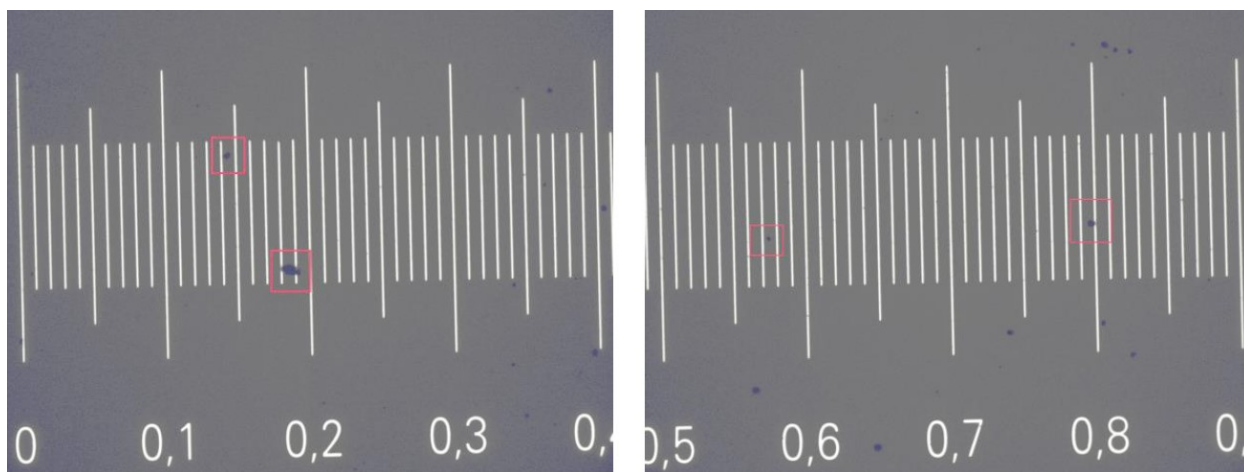


Figure 10 NIM reported two significant faults on line 19 and line 80 in June 2021

A probably non-contamination caused fault was documented by INMETRO in August 2021 in the central part of line 60. This is shown in Figure 11.

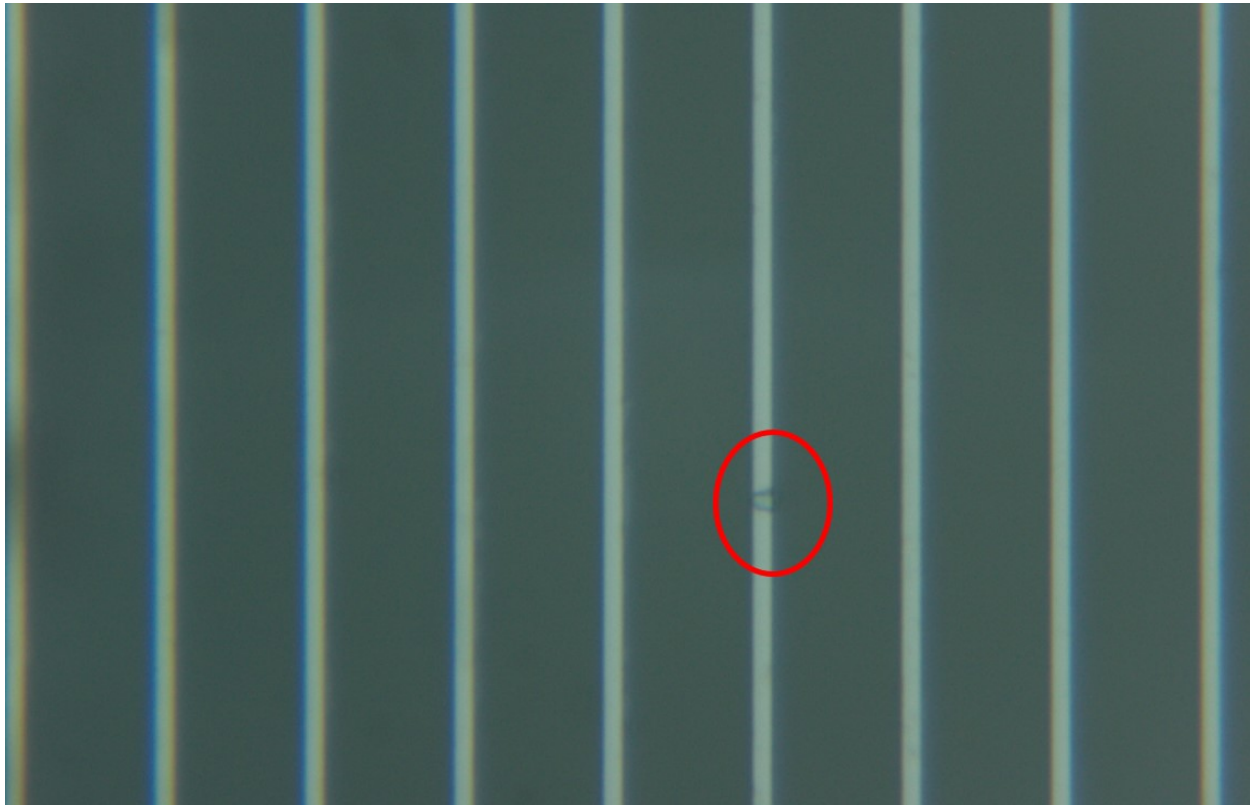


Figure 11 Change on line 60 as documented by INMETRO in August 2021

Overall the participants results did not show a noticeable drift. The stability measurements as outlined in section 4.2 support this finding.

5 Measuring instructions

5.1 Handling the artefact

The technical protocol gives instructions on the handling of the artefact:

“The stage micrometer shall only be handled by authorized persons wearing appropriate gloves. It should be stored in such a way as to prevent damage. The side bearing the graduation should not come in contact with other objects; the transportation box (Figure 4) is constructed in a way to avoid any contact with its walls.

Before making the measurements, the stage micrometer needs to be checked to verify that the measuring surface is not damaged. Micrographic images are the most appropriate way for this check. The condition of the graduation should be documented in the form provided in Appendix B of the technical protocol.

No other measurements are to be attempted by the participants and the stage micrometer should not be used for any purpose other than described in this document. The stage micrometer may not be given to any party other than the participants in the comparison. When not in use, place the scale back into its container to avoid dust or dirt deposits.

The stage micrometer should be examined before despatch and any change in condition during the measurement at each laboratory should be communicated to the pilot laboratory. Ensure that the content of the package is complete before shipment. Always use the original packaging.”

5.2 Cleaning

The technical protocol gives instructions on the cleaning of the artefact:

“The principle rule is not to clean the artefact at all! No cleaning of the scale should be tried besides blowing away dust particles using dry, clean air or other clean gases. Especially, rubbing the surface with soft tissues or any other firm physical contact will possibly damage the line structures of the standards. Application of solvents such as acetone or alcohol is strictly forbidden. If it is necessary to clean the scale before the measurement, please get in contact with the pilot.”

During the course of the comparison CEM noticed an extreme contamination of the artefact. It is speculated that a carrier opened the package in an improper way. CEM got in contact with the pilot and it was tried to clean the stage micrometer using a technique commonly applied for laser resonator mirrors. However, this was unsuccessful and the artefact had to be substituted (see section 4.3).

5.3 Traceability

Length measurements should be traceable to the latest realisation of the metre as set out in the current “*Mise en Pratique*”. Temperature measurements should be made using the International Temperature Scale of 1990 (ITS-90).

5.4 Measurands

The stage micrometer shall be measured based on the standard procedure that the laboratory regularly uses for this calibration service for its customers.

The measurand e_i is the deviation of the distance² l_i between the reference line to the considered line from the nominal distance L_i :

$$e_i = l_i - L_i$$

The distance l_i has to be determined between the center line position of the reference line (zero line, labelled “0”) and the center line position of the measured line. All measurements should be performed over the section of 50 μm width. That is, it should be tried to apply an effective slit height or CCD image window height of 50 μm for the analysis of measurements (Figure 12). This 50 μm window should be positioned symmetrical with respect to the graduation. Since the artefact does not have any guiding structures, there is some arbitrariness in the alignment. This fact and any deviation from the given measurand definition should be recognized by appropriate uncertainty contributions. This decision must be made by the participant (not the pilot).

The measurement results shall be corrected for the reference conditions as stated in section 5.6.

All 100 values e_1 to e_{100} as defined above have to be measured and reported by each participant.

² In the technical protocol this quantity was denoted as d_i . To avoid confusion with the deviation from the SCR, it has been renamed to l_i in this document.

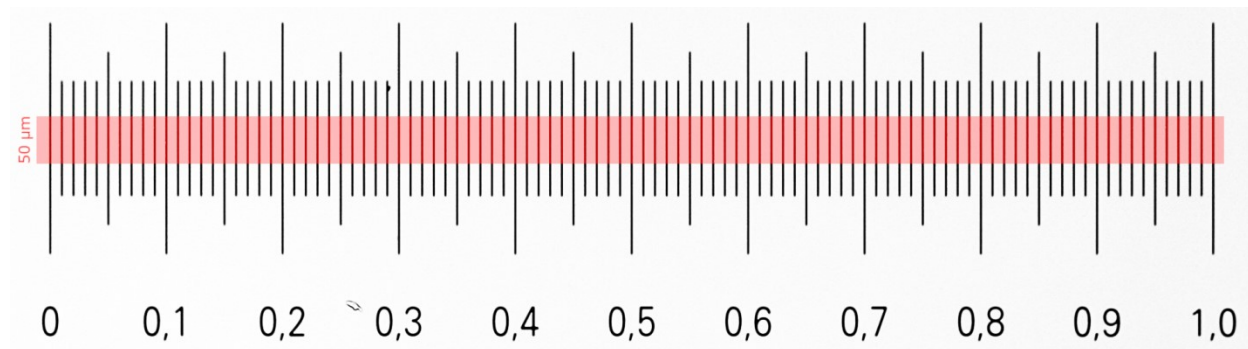


Figure 12 The 50 µm region (in pink) over which the line centers are to be evaluated.

5.5 Measurement uncertainty

The uncertainty of measurement shall be estimated according to the ISO Guide to the Expression of Uncertainty in Measurement. The participating laboratories are encouraged to use their usual model for the uncertainty calculation.

The participants are asked to report the standard uncertainty $u(e_i)$ (or u_i for short) for each of the 100 individual measurement values in the report file. Moreover, the expanded measurement uncertainty U has to be expressed in the usual length-dependent form:

$$U = Q[a, b \cdot L] \equiv \sqrt{a^2 + (b \cdot L)^2}$$

using a coverage factor of $k = 2$.

5.6 Reference condition

Measurement results should be reported for the reference temperature of 20 °C. For corrections, the linear thermal expansion coefficient indicated in section 4.1 should be used. The reference orientation is horizontal with the graduation facing upwards.

6 Results

6.1 Results and standard uncertainties as reported by participants

In the first loop only three NMIs could take part before the respective artefact was destroyed irrecoverably. Table 4 summarizes the results (values and associated standard uncertainties) for each of the participants. As a guide for the eye a plot of the results is presented in Figure 13. Only the values (without uncertainties) are plotted.

In loop 2 the remaining NMIs (11 including BEV) took part calibrating the second artefact. Table 5 summarizes the results (values and associated standard uncertainties) for each of the participants. As a guide for the eye plots of the results are presented in Figure 14 and Figure 15, respectively.

Table 4. Deviation from nominal length (Line deviation, in μm) of the individual scale marks and their standard uncertainties, as reported by the laboratories of loop 1. The order of participants presented in the table heading does not correspond to the chronological order. For chronological order see Table 2.

| Line | INM | | BEV.1 | | GUM | |
|------|------------------------|------------------------|------------------------|------------------------|------------------------|------------------------|
| | e_i μm | u_i μm | e_i μm | u_i μm | e_i μm | u_i μm |
| 1 | -0.240 | 0,500 | -0,001 | 0,024 | 0,017 | 0,045 |
| 2 | 0,100 | 0,500 | -0,005 | 0,024 | 0,013 | 0,045 |
| 3 | 0,210 | 0,500 | 0,015 | 0,024 | 0,046 | 0,045 |
| 4 | 0,050 | 0,500 | 0,014 | 0,024 | 0,034 | 0,045 |
| 5 | -0,230 | 0,500 | 0,012 | 0,024 | 0,044 | 0,045 |
| 6 | -0,090 | 0,500 | 0,011 | 0,024 | 0,035 | 0,045 |
| 7 | -0,140 | 0,500 | 0,011 | 0,024 | 0,045 | 0,045 |
| 8 | -0,110 | 0,500 | 0,011 | 0,024 | 0,046 | 0,045 |
| 9 | -0,140 | 0,500 | 0,009 | 0,024 | 0,045 | 0,045 |
| 10 | -0,110 | 0,500 | 0,012 | 0,024 | 0,033 | 0,045 |
| 11 | -0,030 | 0,500 | 0,025 | 0,024 | 0,059 | 0,045 |
| 12 | -0,120 | 0,500 | 0,024 | 0,024 | 0,055 | 0,045 |
| 13 | -0,150 | 0,500 | 0,020 | 0,024 | 0,054 | 0,045 |
| 14 | -0,260 | 0,500 | 0,019 | 0,024 | 0,046 | 0,045 |
| 15 | -0,220 | 0,510 | 0,015 | 0,024 | 0,048 | 0,045 |
| 16 | -0,080 | 0,510 | 0,014 | 0,024 | 0,041 | 0,045 |
| 17 | -0,220 | 0,510 | 0,014 | 0,024 | 0,046 | 0,045 |
| 18 | -0,300 | 0,510 | 0,014 | 0,024 | 0,043 | 0,045 |
| 19 | 0,820 | 0,510 | 0,023 | 0,024 | 0,057 | 0,045 |
| 20 | -0,020 | 0,510 | 0,022 | 0,024 | 0,045 | 0,045 |
| 21 | -0,320 | 0,510 | 0,023 | 0,024 | 0,062 | 0,045 |
| 22 | -0,240 | 0,510 | 0,026 | 0,024 | 0,049 | 0,045 |
| 23 | -0,340 | 0,510 | 0,023 | 0,024 | 0,055 | 0,045 |
| 24 | -0,420 | 0,510 | 0,026 | 0,024 | 0,051 | 0,045 |
| 25 | -0,500 | 0,520 | 0,023 | 0,024 | 0,057 | 0,045 |
| 26 | -0,350 | 0,520 | 0,023 | 0,024 | 0,047 | 0,045 |
| 27 | -0,300 | 0,520 | 0,027 | 0,024 | 0,054 | 0,045 |
| 28 | -0,170 | 0,520 | 0,029 | 0,024 | 0,046 | 0,045 |
| 29 | -0,230 | 0,520 | 0,027 | 0,024 | 0,058 | 0,045 |
| 30 | -0,150 | 0,520 | 0,028 | 0,024 | 0,044 | 0,045 |
| 31 | -0,250 | 0,520 | 0,012 | 0,024 | 0,044 | 0,045 |
| 32 | -0,170 | 0,520 | 0,010 | 0,024 | 0,036 | 0,045 |
| 33 | -0,110 | 0,530 | 0,011 | 0,024 | 0,049 | 0,045 |
| 34 | -0,220 | 0,530 | 0,012 | 0,024 | 0,039 | 0,045 |
| 35 | -0,340 | 0,530 | 0,012 | 0,024 | 0,046 | 0,045 |
| 36 | -0,300 | 0,530 | 0,014 | 0,024 | 0,050 | 0,045 |
| 37 | -0,220 | 0,530 | 0,013 | 0,024 | 0,048 | 0,045 |
| 38 | -0,070 | 0,530 | 0,010 | 0,024 | 0,036 | 0,045 |
| 39 | -0,110 | 0,540 | 0,013 | 0,024 | 0,039 | 0,045 |
| 40 | -0,110 | 0,540 | 0,013 | 0,024 | 0,042 | 0,045 |
| 41 | -0,220 | 0,540 | 0,014 | 0,024 | 0,039 | 0,045 |
| 42 | -0,130 | 0,540 | 0,014 | 0,024 | 0,042 | 0,045 |
| 43 | -0,210 | 0,540 | 0,012 | 0,024 | 0,040 | 0,045 |
| 44 | -0,090 | 0,550 | 0,012 | 0,024 | 0,040 | 0,045 |
| 45 | -0,250 | 0,550 | 0,011 | 0,024 | 0,037 | 0,045 |
| 46 | -0,230 | 0,550 | 0,012 | 0,024 | 0,023 | 0,045 |
| 47 | -0,300 | 0,550 | 0,017 | 0,024 | 0,041 | 0,045 |
| 48 | -0,480 | 0,550 | 0,018 | 0,024 | 0,042 | 0,045 |
| 49 | -0,320 | 0,560 | 0,017 | 0,024 | 0,041 | 0,045 |
| 50 | -0,330 | 0,560 | 0,013 | 0,024 | 0,031 | 0,045 |
| 51 | -0,190 | 0,560 | 0,019 | 0,024 | 0,037 | 0,045 |
| 52 | -0,260 | 0,560 | 0,017 | 0,024 | 0,028 | 0,045 |
| 53 | -0,170 | 0,570 | 0,015 | 0,024 | 0,029 | 0,045 |
| 54 | -0,130 | 0,570 | 0,018 | 0,024 | 0,031 | 0,045 |
| 55 | -0,120 | 0,570 | 0,023 | 0,024 | 0,029 | 0,045 |
| 56 | -0,260 | 0,570 | 0,022 | 0,024 | 0,031 | 0,045 |
| 57 | -0,220 | 0,580 | 0,019 | 0,024 | 0,025 | 0,045 |
| 58 | -0,150 | 0,580 | 0,016 | 0,024 | 0,027 | 0,045 |
| 59 | 0,000 | 0,580 | 0,018 | 0,024 | 0,013 | 0,045 |
| 60 | -0,110 | 0,580 | 0,016 | 0,024 | 0,014 | 0,045 |
| 61 | -0,270 | 0,590 | 0,016 | 0,024 | 0,013 | 0,045 |
| 62 | -0,230 | 0,590 | 0,019 | 0,024 | 0,024 | 0,045 |
| 63 | -0,200 | 0,590 | 0,027 | 0,024 | 0,015 | 0,045 |
| 64 | -0,230 | 0,590 | 0,026 | 0,024 | 0,033 | 0,045 |
| 65 | -0,260 | 0,600 | 0,024 | 0,024 | 0,018 | 0,045 |
| 66 | -0,200 | 0,600 | 0,025 | 0,024 | 0,011 | 0,045 |
| 67 | -0,160 | 0,600 | 0,026 | 0,024 | 0,016 | 0,045 |
| 68 | -0,240 | 0,600 | 0,025 | 0,024 | 0,021 | 0,045 |
| 69 | -0,030 | 0,610 | 0,025 | 0,024 | 0,013 | 0,045 |
| 70 | -0,280 | 0,610 | 0,028 | 0,024 | 0,019 | 0,045 |
| 71 | -0,310 | 0,610 | 0,038 | 0,024 | 0,029 | 0,045 |
| 72 | -0,320 | 0,620 | 0,037 | 0,024 | 0,034 | 0,045 |
| 73 | -0,110 | 0,620 | 0,034 | 0,024 | 0,018 | 0,045 |
| 74 | -0,180 | 0,620 | 0,031 | 0,024 | 0,016 | 0,045 |
| 75 | -0,030 | 0,620 | 0,028 | 0,024 | 0,008 | 0,045 |
| 76 | -0,190 | 0,630 | 0,030 | 0,024 | 0,017 | 0,045 |
| 77 | -0,020 | 0,630 | 0,026 | 0,024 | 0,003 | 0,045 |
| 78 | -0,430 | 0,630 | 0,033 | 0,024 | 0,018 | 0,045 |
| 79 | -0,100 | 0,640 | 0,038 | 0,024 | 0,011 | 0,045 |
| 80 | -0,180 | 0,640 | 0,037 | 0,024 | 0,026 | 0,045 |
| 81 | -0,160 | 0,640 | 0,037 | 0,024 | 0,016 | 0,045 |
| 82 | -0,070 | 0,650 | 0,044 | 0,024 | 0,021 | 0,045 |
| 83 | -0,040 | 0,650 | 0,042 | 0,024 | 0,011 | 0,045 |
| 84 | -0,040 | 0,650 | 0,040 | 0,024 | 0,019 | 0,045 |
| 85 | -0,050 | 0,660 | 0,041 | 0,024 | 0,005 | 0,045 |
| 86 | -0,050 | 0,660 | 0,041 | 0,024 | 0,026 | 0,045 |
| 87 | 0,020 | 0,660 | 0,039 | 0,024 | 0,015 | 0,045 |
| 88 | -0,020 | 0,670 | 0,041 | 0,024 | 0,017 | 0,045 |
| 89 | 0,050 | 0,670 | 0,039 | 0,024 | 0,004 | 0,045 |
| 90 | 0,000 | 0,670 | 0,023 | 0,024 | -0,011 | 0,045 |
| 91 | -0,020 | 0,680 | 0,021 | 0,024 | -0,022 | 0,045 |
| 92 | 0,040 | 0,680 | 0,021 | 0,024 | -0,014 | 0,045 |
| 93 | -0,140 | 0,680 | 0,019 | 0,024 | -0,014 | 0,045 |
| 94 | -0,050 | 0,690 | 0,023 | 0,024 | -0,014 | 0,045 |
| 95 | 0,020 | 0,690 | 0,022 | 0,024 | -0,016 | 0,045 |
| 96 | 0,170 | 0,690 | 0,023 | 0,024 | -0,015 | 0,045 |
| 97 | 0,150 | 0,700 | 0,023 | 0,024 | -0,015 | 0,045 |
| 98 | 0,010 | 0,700 | 0,025 | 0,024 | -0,005 | 0,045 |
| 99 | 0,110 | 0,700 | 0,024 | 0,024 | -0,018 | 0,045 |
| 100 | 0,030 | 0,710 | 0,024 | 0,024 | -0,012 | 0,045 |

In Tables 4 to 8, the comma is used as the decimal separator instead of the period. This is a consequence of the software used to create them. There should not be any misunderstandings in this context.

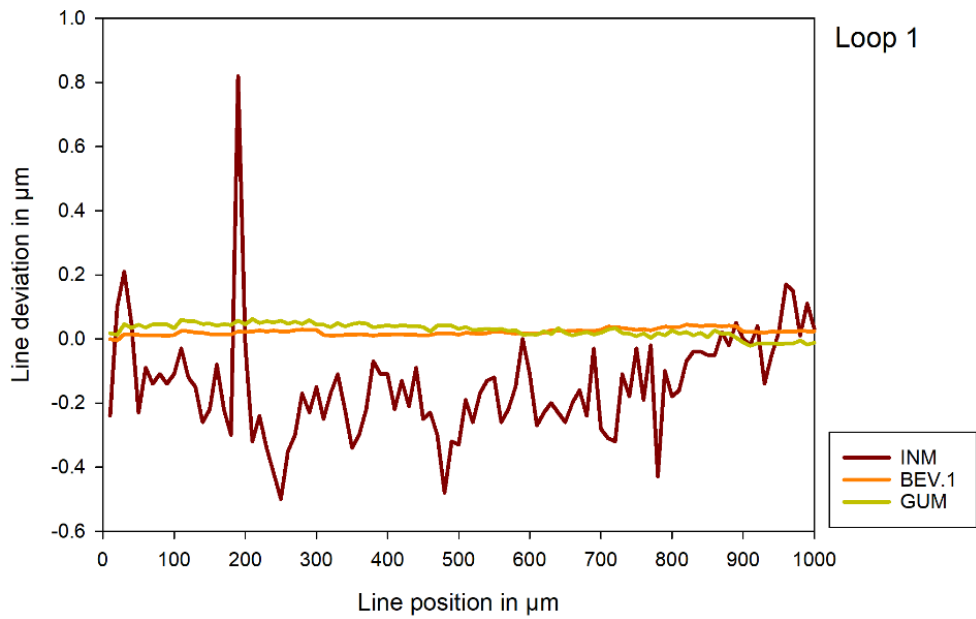


Figure 13 Plot of the results of participants for loop 1. Note the different ordinate scaling as compared to Figure 14 and Figure 15. This is necessary because of the very large deviations of INM as compared to the other participants. The INM results are still in accordance with the SCR_V due to the high expanded measurement uncertainty (up to 1.42 μm).

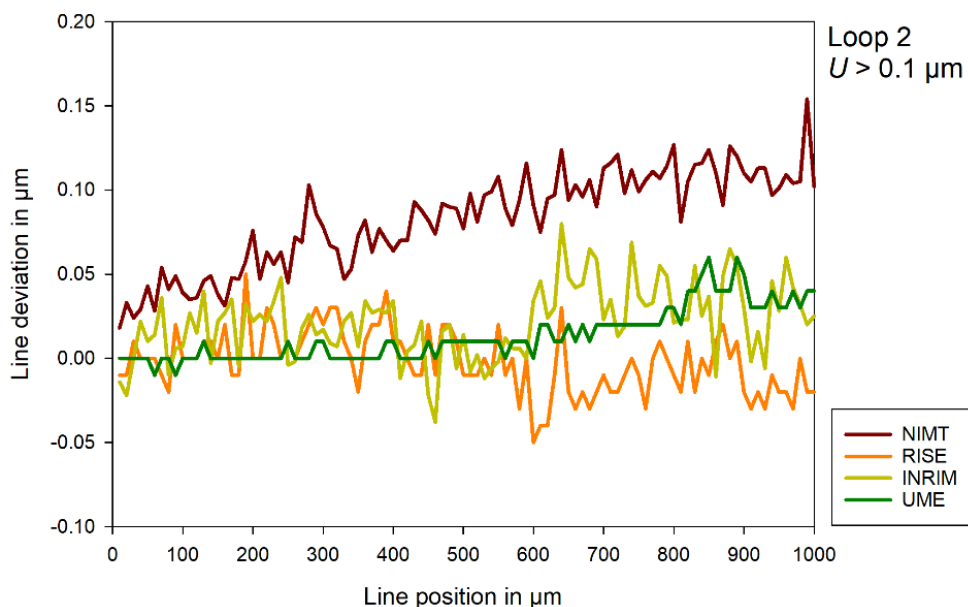


Figure 14 Plot of the results of participants for loop 2. Institutes claiming an expanded uncertainty larger than $0.1 \mu\text{m}$ ($0.18 \mu\text{m}$ to $0.29 \mu\text{m}$).

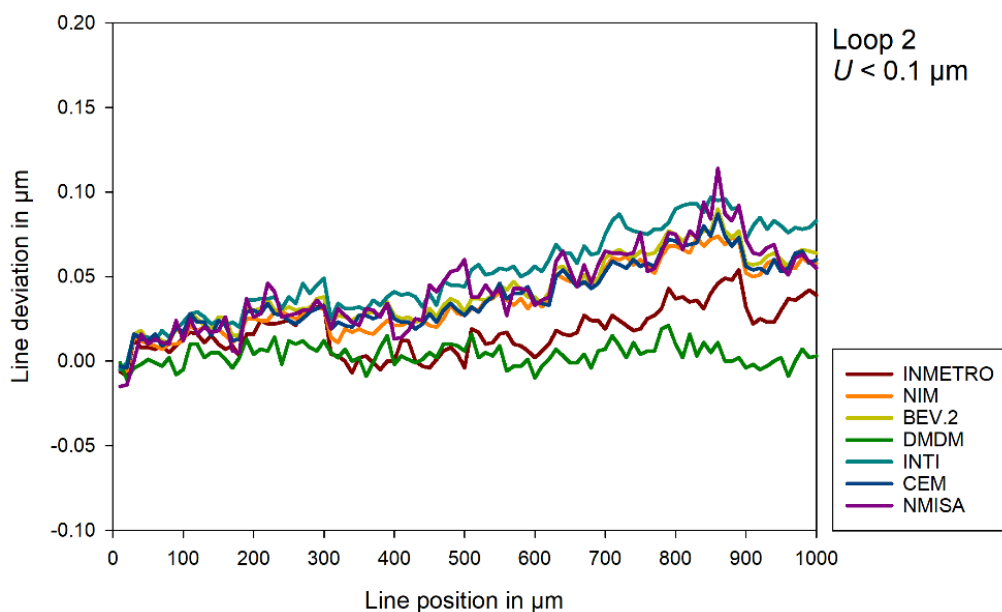


Figure 15 Plot of the results of participants for loop 2. Institutes claiming an expanded uncertainty smaller than $0.1 \mu\text{m}$ ($0.028 \mu\text{m}$ to $0.070 \mu\text{m}$).

6.2 Measurement uncertainties

The participants were asked to submit an overall standard uncertainty value for each of the measurands e_i separately. Moreover, they were asked to submit an uncertainty expression to be comparable to the respective range-based CMC. It was asked for a rounding to the nearest nanometer. It was not required to state the calculated or assumed degrees of freedom.

6.3 Changes to results after Draft A.1

INRIM had reported expanded uncertainties instead of standard uncertainties. By comparison to the published CMC entries this error is plausible.

INMETRO realized a problem with their setup and increased their uncertainty values marginally.

Obviously, these changes caused a slight modification of the reference values, but the overall findings were not affected. No participant showed E_n values large than 1, irrespective of the requested changes.

6.4 Calculation of the SCRv

The technical protocol of this comparison is very specific on the calculation of the reference values and how to treat outliers or other suspicious results. Luckily none of the different measures had to be applied. All results were consistent and no participant stated extremely small or implausible uncertainties. This is quite remarkable since a total of 1400 individual values were subject to the calculation.

The SCRv for each individual line could thus be calculated as the weighted mean of all participants. The procedure was applied for both artefacts separately. A total of 200 SCRv were so obtained, 100 for each artefact.

The total number of participants submitting results is denoted by N (3 for loop 1 and 11 for loop 2). For simplicity no index for the two loops is introduced in the following.

Each laboratory (indexed by j) reports a set of 100 measured values (indexed by i), $e_{i,j}$ and their associated standard uncertainties $u(e_{i,j}) \equiv u_{i,j}$.

The normalised weights, $w_{i,j}$, for the results $e_{i,j}$, are given by:

$$w_{i,j} = \frac{C_i}{u_{i,j}^2}$$

Where the normalising factors, C_i , are given by:

$$C_i = \sum_{j=1}^N \frac{1}{u_{i,j}^2}$$

Using the normalized weights the reference values for each line are the weighted means, $e_{i,\text{ref}}$, which are given by:

$$e_{i,\text{ref}} = \sum_{j=1}^N w_{i,j} \cdot e_{i,j}$$

The associated standard uncertainties of the reference values are calculated by:

$$u_{i,\text{ref}} = \sqrt{C_i}$$

The reference values and their associated standard uncertainties for both loops are compiled in Table 6 and Figure 16, respectively.

Table 6 Supplementary comparison reference values (SCRV) for both artefacts and for each line

| Line | SCRV loop 1 | | Line | SCRV loop 2 | |
|------|------------------|------------------|------|------------------|------------------|
| | e_{Lref} μm | u_{Lref} μm | | e_{Lref} μm | u_{Lref} μm |
| 1 | 0,002 | 0,021 | 1 | -0,005 | 0,008 |
| 2 | -0,001 | 0,021 | 2 | -0,007 | 0,008 |
| 3 | 0,022 | 0,021 | 3 | 0,012 | 0,008 |
| 4 | 0,019 | 0,021 | 4 | 0,012 | 0,008 |
| 5 | 0,019 | 0,021 | 5 | 0,010 | 0,008 |
| 6 | 0,016 | 0,021 | 6 | 0,010 | 0,008 |
| 7 | 0,018 | 0,021 | 7 | 0,009 | 0,008 |
| 8 | 0,019 | 0,021 | 8 | 0,009 | 0,008 |
| 9 | 0,017 | 0,021 | 9 | 0,012 | 0,008 |
| 10 | 0,016 | 0,021 | 10 | 0,013 | 0,008 |
| 11 | 0,032 | 0,021 | 11 | 0,022 | 0,008 |
| 12 | 0,031 | 0,021 | 12 | 0,019 | 0,008 |
| 13 | 0,027 | 0,021 | 13 | 0,018 | 0,008 |
| 14 | 0,024 | 0,021 | 14 | 0,017 | 0,008 |
| 15 | 0,022 | 0,021 | 15 | 0,018 | 0,008 |
| 16 | 0,020 | 0,021 | 16 | 0,015 | 0,009 |
| 17 | 0,021 | 0,021 | 17 | 0,011 | 0,008 |
| 18 | 0,020 | 0,021 | 18 | 0,011 | 0,008 |
| 19 | 0,032 | 0,021 | 19 | 0,026 | 0,008 |
| 20 | 0,027 | 0,021 | 20 | 0,024 | 0,008 |
| 21 | 0,031 | 0,021 | 21 | 0,025 | 0,008 |
| 22 | 0,031 | 0,021 | 22 | 0,027 | 0,009 |
| 23 | 0,029 | 0,021 | 23 | 0,028 | 0,008 |
| 24 | 0,031 | 0,021 | 24 | 0,026 | 0,008 |
| 25 | 0,030 | 0,021 | 25 | 0,026 | 0,008 |
| 26 | 0,027 | 0,021 | 26 | 0,024 | 0,008 |
| 27 | 0,032 | 0,021 | 27 | 0,028 | 0,008 |
| 28 | 0,032 | 0,021 | 28 | 0,030 | 0,008 |
| 29 | 0,033 | 0,021 | 29 | 0,031 | 0,008 |
| 30 | 0,031 | 0,021 | 30 | 0,032 | 0,008 |
| 31 | 0,019 | 0,021 | 31 | 0,015 | 0,008 |
| 32 | 0,016 | 0,021 | 32 | 0,015 | 0,008 |
| 33 | 0,019 | 0,021 | 33 | 0,017 | 0,008 |
| 34 | 0,018 | 0,021 | 34 | 0,014 | 0,008 |
| 35 | 0,019 | 0,021 | 35 | 0,018 | 0,008 |
| 36 | 0,021 | 0,021 | 36 | 0,017 | 0,008 |
| 37 | 0,020 | 0,021 | 37 | 0,017 | 0,008 |
| 38 | 0,016 | 0,021 | 38 | 0,018 | 0,008 |
| 39 | 0,019 | 0,021 | 39 | 0,022 | 0,009 |
| 40 | 0,019 | 0,021 | 40 | 0,018 | 0,008 |
| 41 | 0,019 | 0,021 | 41 | 0,019 | 0,008 |
| 42 | 0,020 | 0,021 | 42 | 0,020 | 0,008 |
| 43 | 0,018 | 0,021 | 43 | 0,018 | 0,008 |
| 44 | 0,018 | 0,021 | 44 | 0,018 | 0,008 |
| 45 | 0,017 | 0,021 | 45 | 0,020 | 0,008 |
| 46 | 0,014 | 0,021 | 46 | 0,018 | 0,008 |
| 47 | 0,022 | 0,021 | 47 | 0,025 | 0,008 |
| 48 | 0,022 | 0,021 | 48 | 0,029 | 0,008 |
| 49 | 0,022 | 0,021 | 49 | 0,026 | 0,008 |
| 50 | 0,016 | 0,021 | 50 | 0,023 | 0,008 |
| 51 | 0,023 | 0,021 | 51 | 0,030 | 0,008 |
| 52 | 0,019 | 0,021 | 52 | 0,029 | 0,008 |
| 53 | 0,018 | 0,021 | 53 | 0,030 | 0,008 |
| 54 | 0,021 | 0,021 | 54 | 0,031 | 0,008 |
| 55 | 0,024 | 0,021 | 55 | 0,036 | 0,008 |
| 56 | 0,024 | 0,021 | 56 | 0,031 | 0,008 |
| 57 | 0,020 | 0,021 | 57 | 0,031 | 0,008 |
| 58 | 0,018 | 0,021 | 58 | 0,031 | 0,008 |
| 59 | 0,017 | 0,021 | 59 | 0,029 | 0,008 |
| 60 | 0,016 | 0,021 | 60 | 0,028 | 0,008 |
| 61 | 0,015 | 0,021 | 61 | 0,027 | 0,008 |
| 62 | 0,020 | 0,021 | 62 | 0,031 | 0,008 |
| 63 | 0,024 | 0,021 | 63 | 0,044 | 0,008 |
| 64 | 0,027 | 0,021 | 64 | 0,044 | 0,008 |
| 65 | 0,022 | 0,021 | 65 | 0,040 | 0,008 |
| 66 | 0,021 | 0,021 | 66 | 0,038 | 0,008 |
| 67 | 0,023 | 0,021 | 67 | 0,042 | 0,008 |
| 68 | 0,024 | 0,021 | 68 | 0,040 | 0,008 |
| 69 | 0,022 | 0,021 | 69 | 0,042 | 0,008 |
| 70 | 0,025 | 0,021 | 70 | 0,047 | 0,008 |
| 71 | 0,036 | 0,021 | 71 | 0,053 | 0,008 |
| 72 | 0,036 | 0,021 | 72 | 0,052 | 0,008 |
| 73 | 0,030 | 0,021 | 73 | 0,050 | 0,008 |
| 74 | 0,027 | 0,021 | 74 | 0,049 | 0,008 |
| 75 | 0,024 | 0,021 | 75 | 0,051 | 0,008 |
| 76 | 0,027 | 0,021 | 76 | 0,049 | 0,008 |
| 77 | 0,021 | 0,021 | 77 | 0,048 | 0,008 |
| 78 | 0,029 | 0,021 | 78 | 0,056 | 0,008 |
| 79 | 0,032 | 0,021 | 79 | 0,062 | 0,009 |
| 80 | 0,034 | 0,021 | 80 | 0,061 | 0,008 |
| 81 | 0,032 | 0,021 | 81 | 0,058 | 0,008 |
| 82 | 0,039 | 0,021 | 82 | 0,060 | 0,008 |
| 83 | 0,035 | 0,021 | 83 | 0,062 | 0,008 |
| 84 | 0,035 | 0,021 | 84 | 0,063 | 0,008 |
| 85 | 0,033 | 0,021 | 85 | 0,065 | 0,008 |
| 86 | 0,038 | 0,021 | 86 | 0,070 | 0,009 |
| 87 | 0,033 | 0,021 | 87 | 0,065 | 0,008 |
| 88 | 0,036 | 0,021 | 88 | 0,065 | 0,008 |
| 89 | 0,031 | 0,021 | 89 | 0,067 | 0,008 |
| 90 | 0,015 | 0,021 | 90 | 0,048 | 0,008 |
| 91 | 0,011 | 0,021 | 91 | 0,045 | 0,008 |
| 92 | 0,014 | 0,021 | 92 | 0,046 | 0,008 |
| 93 | 0,012 | 0,021 | 93 | 0,048 | 0,008 |
| 94 | 0,014 | 0,021 | 94 | 0,052 | 0,008 |
| 95 | 0,014 | 0,021 | 95 | 0,050 | 0,008 |
| 96 | 0,014 | 0,021 | 96 | 0,049 | 0,008 |
| 97 | 0,015 | 0,021 | 97 | 0,051 | 0,008 |
| 98 | 0,018 | 0,021 | 98 | 0,055 | 0,008 |
| 99 | 0,015 | 0,021 | 99 | 0,053 | 0,008 |
| 100 | 0,016 | 0,021 | 100 | 0,053 | 0,008 |

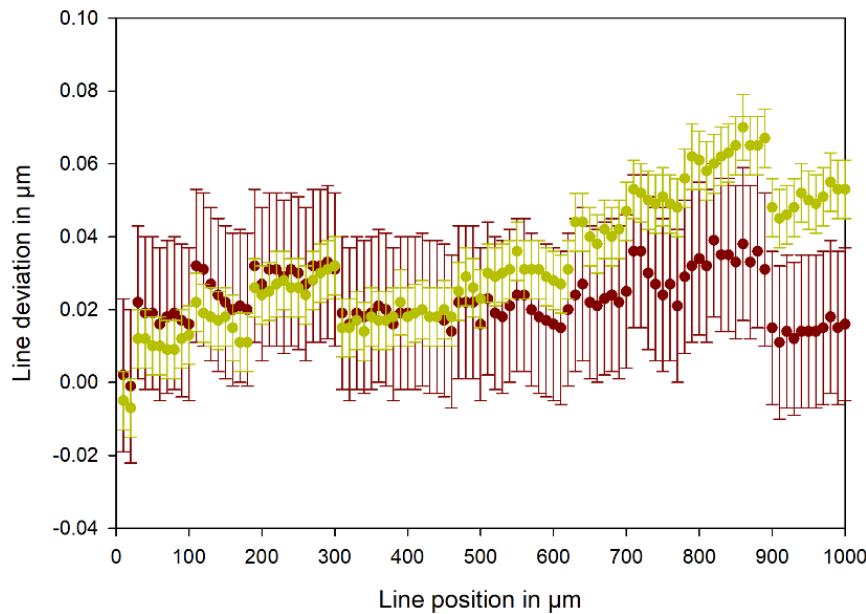


Figure 16 Reference values (SCRV) for the two artefacts used in the two loops. Red symbols for loop 1, green symbols for loop 2. Error bars denote the standard uncertainties of the reference values.

6.5 Calculation of Degrees of Equivalence

The Degree of Equivalence, DoE, for a laboratory result is simply the difference of each laboratory's result from the reference values. For each laboratory there exist 100 DoE. They are denoted by $d_{i,j}$:

$$d_{i,j} = e_{i,j} - e_{i,\text{ref}}$$

Since all results contributed to the weighted mean, their associated standard uncertainty is given by:

$$u(d_{i,j}) = \sqrt{u_{i,j}^2 - u_{i,\text{ref}}^2}$$

The minus sign reflects the impact of correlation between the individual deviations and the reference deviation, calculated from all individual deviations for each line position.

Finally, the deviations normalized to their expanded uncertainties (E_n , assuming $k = 2$) are determined for each laboratory j and each line i by:

$$E_{n\ i,j} = \frac{d_{i,j}}{2 u(d_{i,j})}$$

The calculated results (DoE) for the participants are presented in Table 7 (for loop 1) and Table 8 (for loop 2), respectively. Table 9 summarized the absolute E_n values for all participants.

6.5.1 Tabular representation of DoE results

Table 7 Degree of equivalence (DoE) with standard uncertainties for the participants of loop 1. The order of participants presented in the table heading does not correspond to the chronological order. For chronological order see Table 2.

| Line | INM | | BEV.1 | | GUM | |
|------|-------------|----------------|-------------|----------------|-------------|----------------|
| | d_i μm | $u(d_i)$ μm | d_i μm | $u(d_i)$ μm | d_i μm | $u(d_i)$ μm |
| 1 | -0,242 | 0,500 | -0,004 | 0,011 | 0,015 | 0,040 |
| 2 | 0,101 | 0,500 | -0,004 | 0,011 | 0,014 | 0,040 |
| 3 | 0,188 | 0,500 | -0,007 | 0,011 | 0,024 | 0,040 |
| 4 | 0,031 | 0,500 | -0,004 | 0,011 | 0,015 | 0,040 |
| 5 | -0,249 | 0,500 | -0,007 | 0,011 | 0,025 | 0,040 |
| 6 | -0,106 | 0,500 | -0,005 | 0,011 | 0,019 | 0,040 |
| 7 | -0,158 | 0,500 | -0,007 | 0,011 | 0,027 | 0,040 |
| 8 | -0,129 | 0,500 | -0,008 | 0,011 | 0,027 | 0,040 |
| 9 | -0,157 | 0,500 | -0,008 | 0,011 | 0,028 | 0,040 |
| 10 | -0,126 | 0,500 | -0,004 | 0,011 | 0,017 | 0,040 |
| 11 | -0,062 | 0,500 | -0,007 | 0,011 | 0,027 | 0,040 |
| 12 | -0,151 | 0,500 | -0,007 | 0,011 | 0,024 | 0,040 |
| 13 | -0,177 | 0,500 | -0,007 | 0,011 | 0,027 | 0,040 |
| 14 | -0,284 | 0,500 | -0,005 | 0,011 | 0,022 | 0,040 |
| 15 | -0,242 | 0,510 | -0,007 | 0,011 | 0,026 | 0,040 |
| 16 | -0,100 | 0,510 | -0,006 | 0,011 | 0,021 | 0,040 |
| 17 | -0,241 | 0,510 | -0,007 | 0,011 | 0,025 | 0,040 |
| 18 | -0,320 | 0,510 | -0,006 | 0,011 | 0,023 | 0,040 |
| 19 | 0,788 | 0,510 | -0,009 | 0,011 | 0,025 | 0,040 |
| 20 | -0,047 | 0,510 | -0,005 | 0,011 | 0,018 | 0,040 |
| 21 | -0,351 | 0,510 | -0,008 | 0,011 | 0,031 | 0,040 |
| 22 | -0,271 | 0,510 | -0,005 | 0,011 | 0,018 | 0,040 |
| 23 | -0,369 | 0,510 | -0,007 | 0,011 | 0,026 | 0,040 |
| 24 | -0,451 | 0,510 | -0,005 | 0,011 | 0,020 | 0,040 |
| 25 | -0,530 | 0,520 | -0,007 | 0,011 | 0,027 | 0,040 |
| 26 | -0,377 | 0,520 | -0,005 | 0,011 | 0,020 | 0,040 |
| 27 | -0,332 | 0,520 | -0,005 | 0,011 | 0,022 | 0,040 |
| 28 | -0,202 | 0,520 | -0,003 | 0,011 | 0,014 | 0,040 |
| 29 | -0,263 | 0,520 | -0,006 | 0,011 | 0,025 | 0,040 |
| 30 | -0,181 | 0,520 | -0,003 | 0,011 | 0,013 | 0,040 |
| 31 | -0,269 | 0,520 | -0,007 | 0,011 | 0,025 | 0,040 |
| 32 | -0,186 | 0,520 | -0,005 | 0,011 | 0,020 | 0,040 |
| 33 | -0,129 | 0,530 | -0,008 | 0,011 | 0,030 | 0,040 |
| 34 | -0,238 | 0,530 | -0,006 | 0,011 | 0,021 | 0,040 |
| 35 | -0,359 | 0,530 | -0,007 | 0,011 | 0,027 | 0,040 |
| 36 | -0,321 | 0,530 | -0,007 | 0,011 | 0,029 | 0,040 |
| 37 | -0,240 | 0,530 | -0,007 | 0,011 | 0,028 | 0,040 |
| 38 | -0,086 | 0,530 | -0,006 | 0,011 | 0,020 | 0,040 |
| 39 | -0,129 | 0,540 | -0,005 | 0,011 | 0,020 | 0,040 |
| 40 | -0,129 | 0,540 | -0,006 | 0,011 | 0,023 | 0,040 |
| 41 | -0,239 | 0,540 | -0,005 | 0,011 | 0,020 | 0,040 |
| 42 | -0,150 | 0,540 | -0,006 | 0,011 | 0,022 | 0,040 |
| 43 | -0,228 | 0,540 | -0,006 | 0,011 | 0,022 | 0,040 |
| 44 | -0,108 | 0,550 | -0,006 | 0,011 | 0,022 | 0,040 |
| 45 | -0,267 | 0,550 | -0,005 | 0,011 | 0,020 | 0,040 |
| 46 | -0,244 | 0,550 | -0,002 | 0,011 | 0,009 | 0,040 |
| 47 | -0,322 | 0,550 | -0,005 | 0,011 | 0,019 | 0,040 |
| 48 | -0,502 | 0,550 | -0,005 | 0,011 | 0,020 | 0,040 |
| 49 | -0,342 | 0,560 | -0,005 | 0,011 | 0,019 | 0,040 |
| 50 | -0,346 | 0,560 | -0,004 | 0,011 | 0,015 | 0,040 |
| 51 | -0,213 | 0,560 | -0,004 | 0,011 | 0,014 | 0,040 |
| 52 | -0,279 | 0,560 | -0,002 | 0,011 | 0,009 | 0,040 |
| 53 | -0,188 | 0,570 | -0,003 | 0,011 | 0,011 | 0,040 |
| 54 | -0,151 | 0,570 | -0,003 | 0,011 | 0,010 | 0,040 |
| 55 | -0,144 | 0,570 | -0,001 | 0,011 | 0,005 | 0,040 |
| 56 | -0,284 | 0,570 | -0,002 | 0,011 | 0,007 | 0,040 |
| 57 | -0,240 | 0,580 | -0,001 | 0,011 | 0,005 | 0,040 |
| 58 | -0,168 | 0,580 | -0,002 | 0,011 | 0,009 | 0,040 |
| 59 | -0,017 | 0,580 | 0,001 | 0,011 | -0,004 | 0,040 |
| 60 | -0,126 | 0,580 | 0,001 | 0,011 | -0,002 | 0,040 |
| 61 | -0,285 | 0,590 | 0,001 | 0,011 | -0,002 | 0,040 |
| 62 | -0,250 | 0,590 | -0,001 | 0,011 | 0,004 | 0,040 |
| 63 | -0,224 | 0,590 | 0,003 | 0,011 | -0,009 | 0,040 |
| 64 | -0,257 | 0,590 | -0,001 | 0,011 | 0,006 | 0,040 |
| 65 | -0,282 | 0,600 | 0,002 | 0,011 | 0,004 | 0,040 |
| 66 | -0,221 | 0,600 | 0,003 | 0,011 | -0,010 | 0,040 |
| 67 | -0,183 | 0,600 | 0,002 | 0,011 | -0,007 | 0,040 |
| 68 | -0,264 | 0,600 | 0,001 | 0,011 | -0,003 | 0,040 |
| 69 | -0,052 | 0,610 | 0,003 | 0,011 | -0,009 | 0,040 |
| 70 | -0,305 | 0,610 | 0,002 | 0,011 | -0,006 | 0,040 |
| 71 | -0,346 | 0,610 | 0,003 | 0,011 | -0,007 | 0,040 |
| 72 | -0,356 | 0,620 | 0,001 | 0,011 | -0,002 | 0,040 |
| 73 | -0,140 | 0,620 | 0,004 | 0,011 | -0,012 | 0,040 |
| 74 | -0,207 | 0,620 | 0,004 | 0,011 | -0,011 | 0,040 |
| 75 | -0,054 | 0,620 | 0,005 | 0,011 | -0,016 | 0,040 |
| 76 | -0,217 | 0,630 | 0,003 | 0,011 | -0,010 | 0,040 |
| 77 | -0,041 | 0,630 | 0,005 | 0,011 | -0,018 | 0,040 |
| 78 | -0,459 | 0,630 | 0,004 | 0,011 | -0,011 | 0,040 |
| 79 | -0,132 | 0,640 | 0,006 | 0,011 | -0,021 | 0,040 |
| 80 | -0,214 | 0,640 | 0,003 | 0,011 | -0,008 | 0,040 |
| 81 | -0,192 | 0,640 | 0,005 | 0,011 | -0,016 | 0,040 |
| 82 | -0,109 | 0,650 | 0,005 | 0,011 | -0,018 | 0,040 |
| 83 | -0,075 | 0,650 | 0,007 | 0,011 | -0,024 | 0,040 |
| 84 | -0,075 | 0,650 | 0,005 | 0,011 | -0,016 | 0,040 |
| 85 | -0,083 | 0,660 | 0,008 | 0,011 | -0,028 | 0,040 |
| 86 | -0,088 | 0,660 | 0,003 | 0,011 | -0,012 | 0,040 |
| 87 | -0,013 | 0,660 | 0,005 | 0,011 | -0,018 | 0,040 |
| 88 | -0,056 | 0,670 | 0,005 | 0,011 | -0,019 | 0,040 |
| 89 | 0,019 | 0,670 | 0,008 | 0,011 | -0,027 | 0,040 |
| 90 | -0,015 | 0,670 | 0,008 | 0,011 | -0,026 | 0,040 |
| 91 | -0,031 | 0,680 | 0,009 | 0,011 | -0,033 | 0,040 |
| 92 | 0,026 | 0,680 | 0,008 | 0,011 | -0,028 | 0,040 |
| 93 | -0,152 | 0,680 | 0,007 | 0,011 | -0,026 | 0,040 |
| 94 | -0,064 | 0,690 | 0,008 | 0,011 | -0,028 | 0,040 |
| 95 | 0,006 | 0,690 | 0,009 | 0,011 | -0,030 | 0,040 |
| 96 | 0,156 | 0,690 | 0,008 | 0,011 | -0,029 | 0,040 |
| 97 | 0,135 | 0,700 | 0,008 | 0,011 | -0,030 | 0,040 |
| 98 | -0,008 | 0,700 | 0,007 | 0,011 | -0,023 | 0,040 |
| 99 | 0,095 | 0,700 | 0,009 | 0,011 | -0,033 | 0,040 |
| 100 | 0,014 | 0,710 | 0,008 | 0,011 | -0,028 | 0,040 |

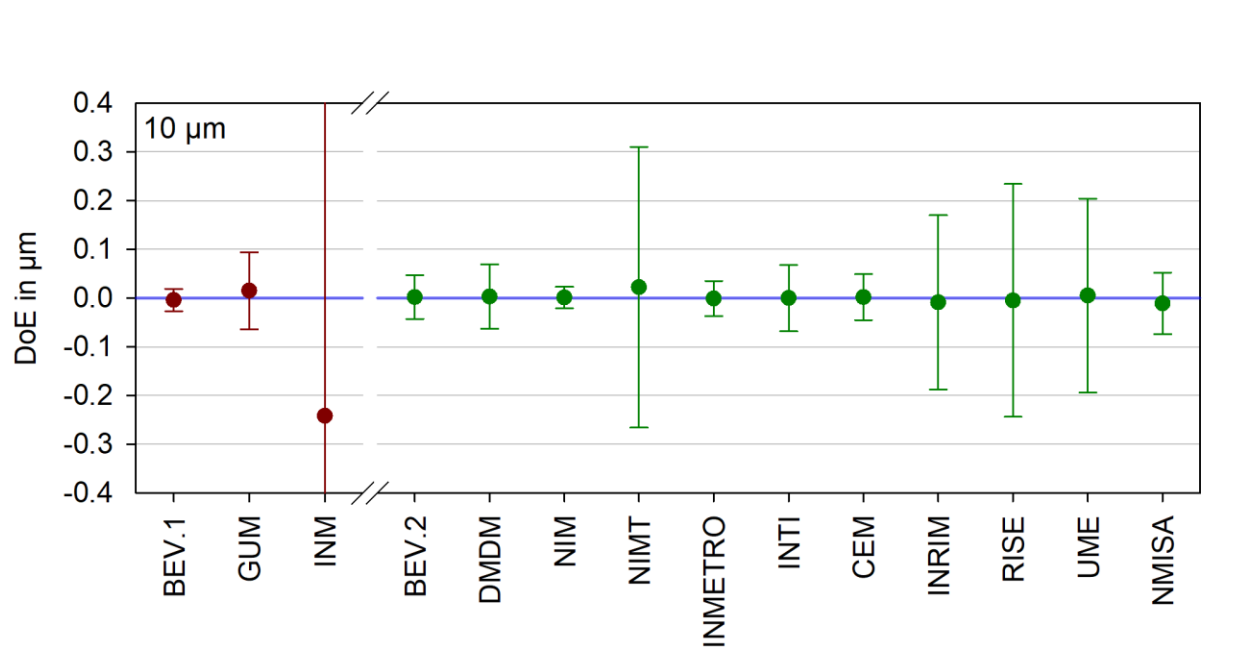


Figure 17 Degree of equivalence (d_1) of all participants for the line mark 10 µm. The error bars denote the expanded measurement uncertainty $U(d_1)$ for $k = 2$. Red symbols (left to axis break) for results of participants of loop 1, green symbols (right to axis break) for results of participants of loop 2. Error bars for INM are too large for the chosen scale.

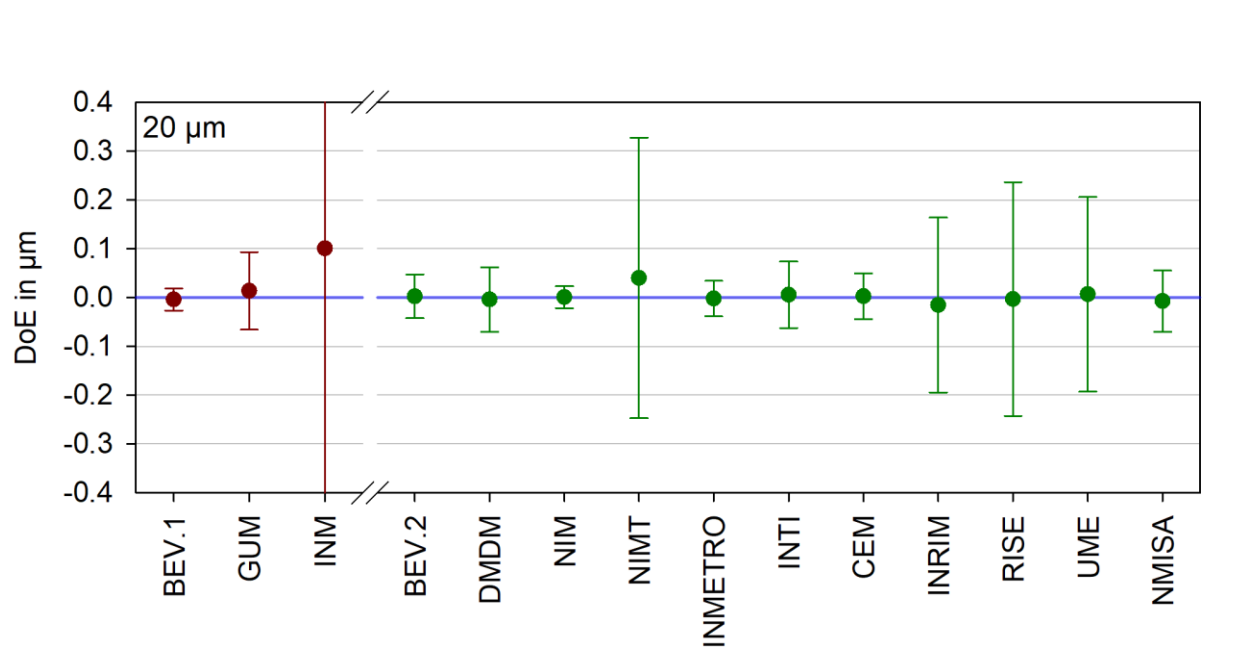


Figure 18 Degree of equivalence (d_2) of all participants for the line mark 20 µm. The error bars denote the expanded measurement uncertainty $U(d_2)$ for $k = 2$. Red symbols (left to axis break) for results of participants of loop 1, green symbols (right to axis break) for results of participants of loop 2. Error bars for INM are too large for the chosen scale.

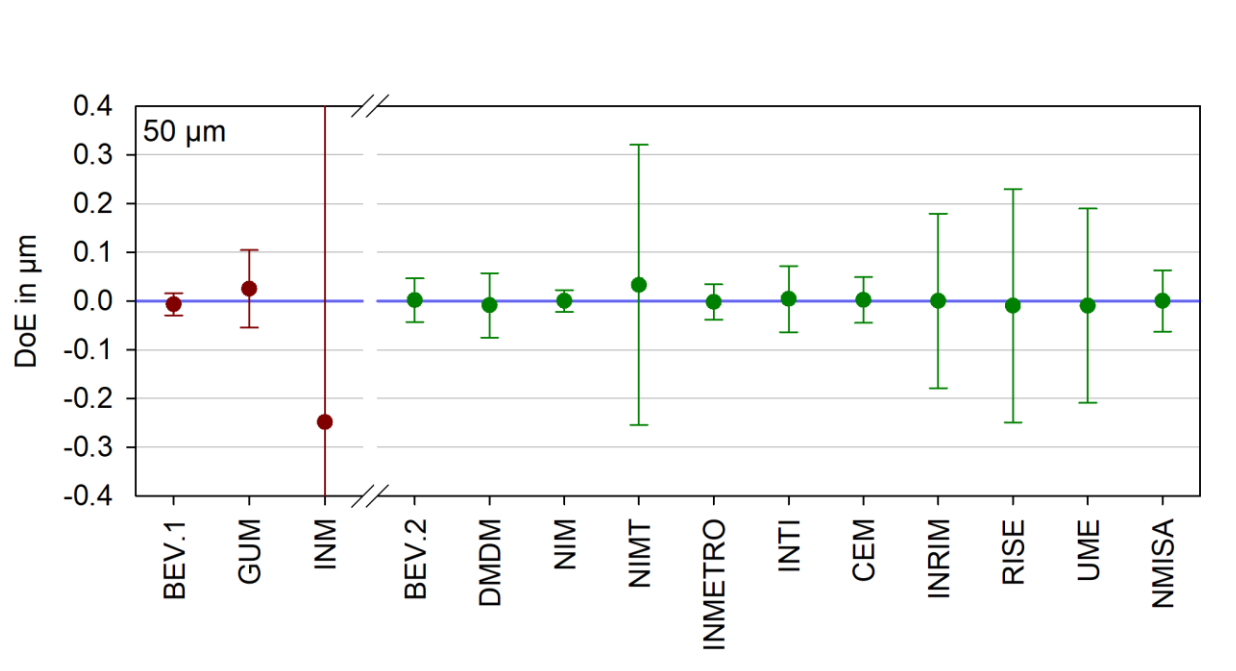


Figure 19 Degree of equivalence (d_s) of all participants for the line mark 50 µm. The error bars denote the expanded measurement uncertainty $U(d_s)$ for $k = 2$. Red symbols (left to axis break) for results of participants of loop 1, green symbols (right to axis break) for results of participants of loop 2. Error bars for INM are too large for the chosen scale.

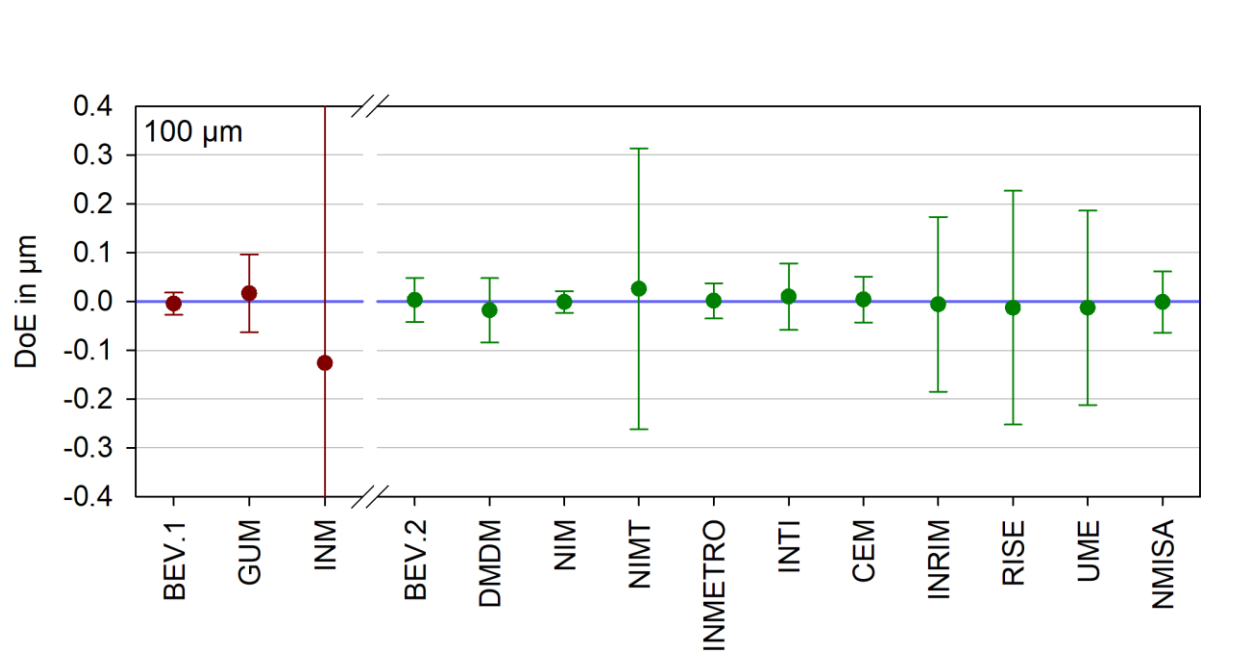


Figure 20 Degree of equivalence (d_{10}) of all participants for the line mark 100 µm. The error bars denote the expanded measurement uncertainty $U(d_{10})$ for $k = 2$. Red symbols (left to axis break) for results of participants of loop 1, green symbols (right to axis break) for results of participants of loop 2. Error bars for INM are too large for the chosen scale.

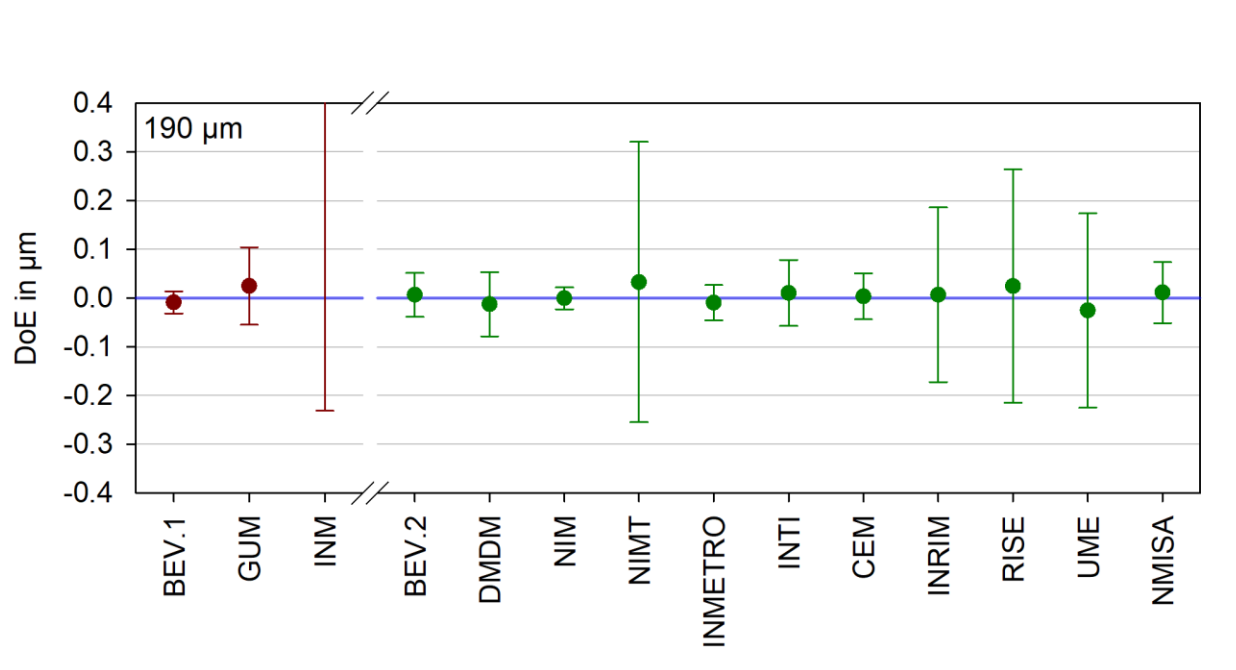


Figure 21 Degree of equivalence (d_{19}) of all participants for the line mark $190 \mu\text{m}$. The error bars denote the expanded measurement uncertainty $U(d_{19})$ for $k = 2$. Red symbols (left to axis break), green symbols (right to axis break) for results of participants of loop 1, green symbols (right to axis break) for results of participants of loop 2. Error bars for INM are too large for the chosen scale.

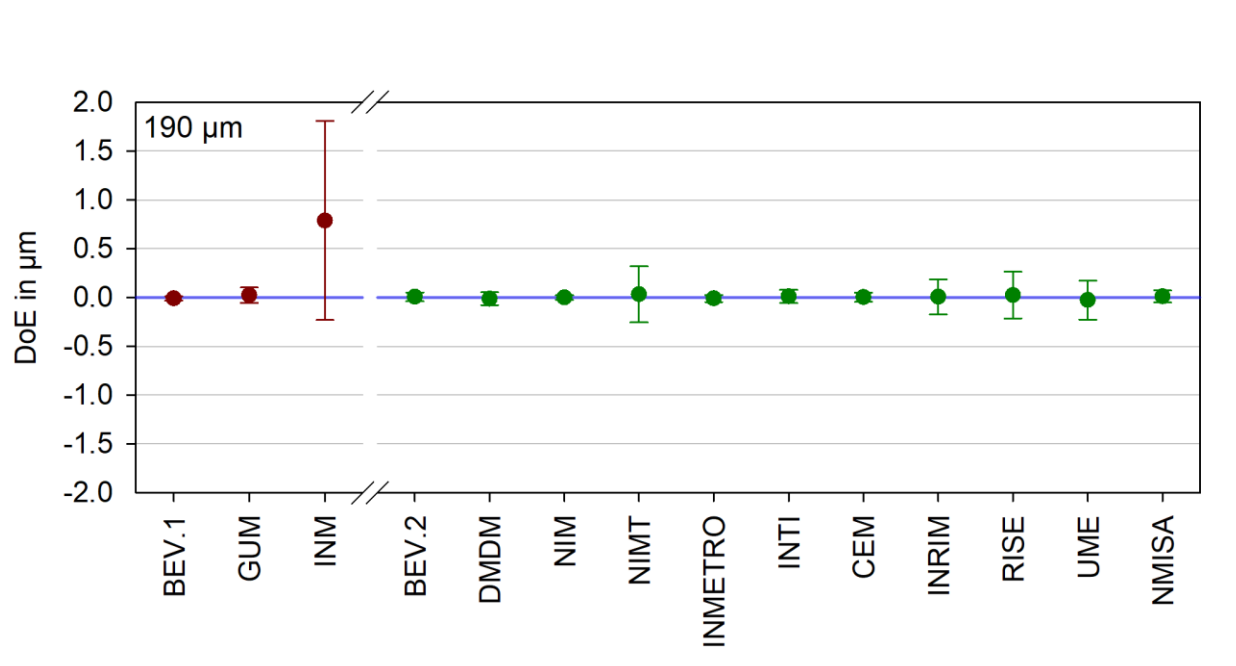


Figure 22 Degree of equivalence (d_{19}) of all participants for the line mark $190 \mu\text{m}$. Same data as of Figure 21 with expanded ordinate scale to visualize INM value.

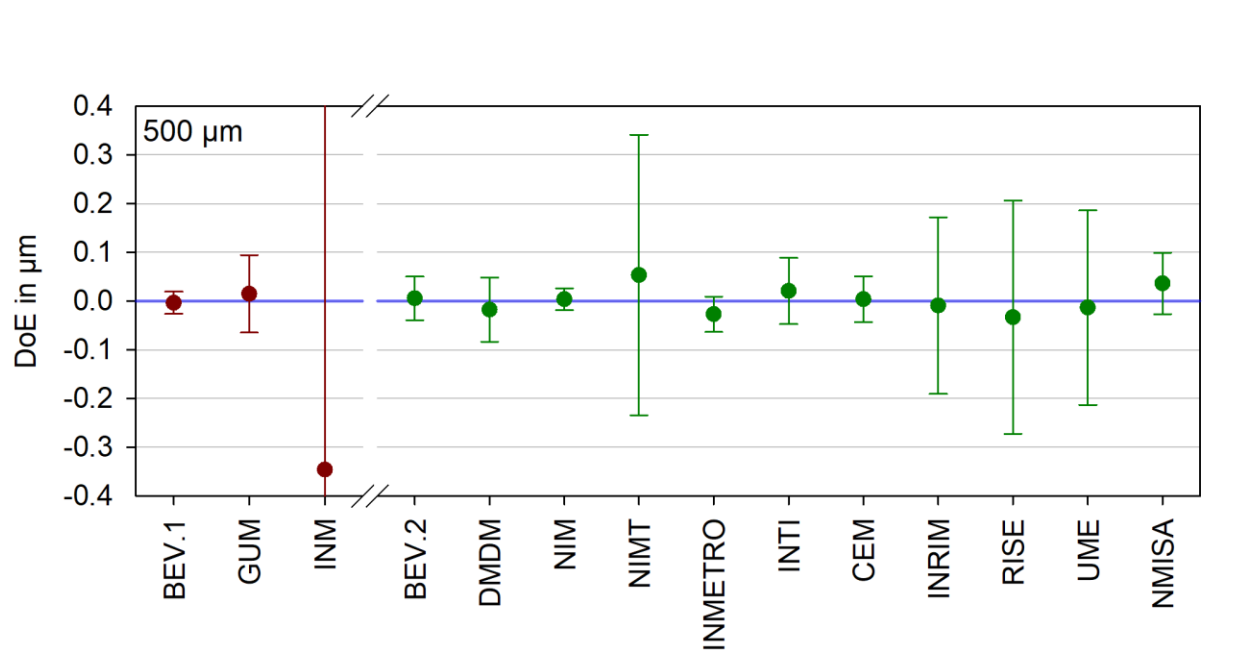


Figure 23 Degree of equivalence (d_{50}) of all participants for the line mark 500 μm . The error bars denote the expanded measurement uncertainty $U(d_{50})$ for $k = 2$. Red symbols (left to axis break) for results of participants of loop 1, green symbols (right to axis break) for results of participants of loop 2. Error bars for INM are too large for the chosen scale.

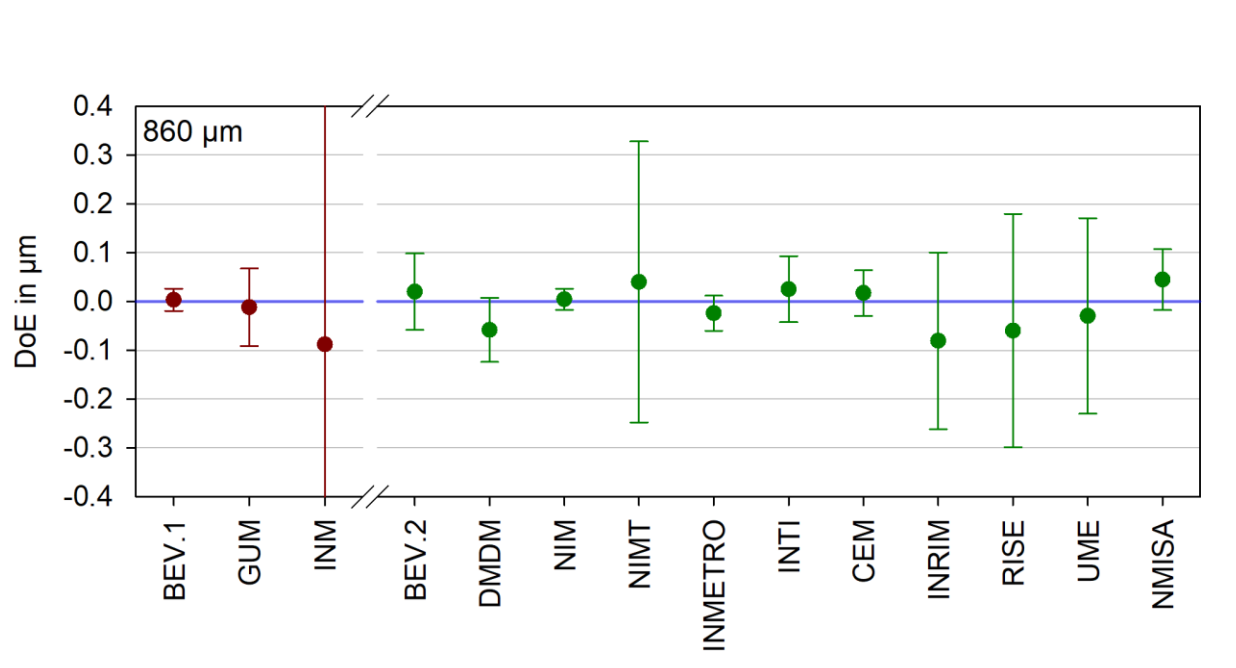


Figure 24 Degree of equivalence (d_{86}) of all participants for the line mark 860 μm . The error bars denote the expanded measurement uncertainty $U(d_{86})$ for $k = 2$. Red symbols (left to axis break) for results of participants of loop 1, green symbols (right to axis break) for results of participants of loop 2. Error bars for INM are too large for the chosen scale. For loop 2 some participants reported a worse line quality at 860 μm . The results also show considerably higher scatter.

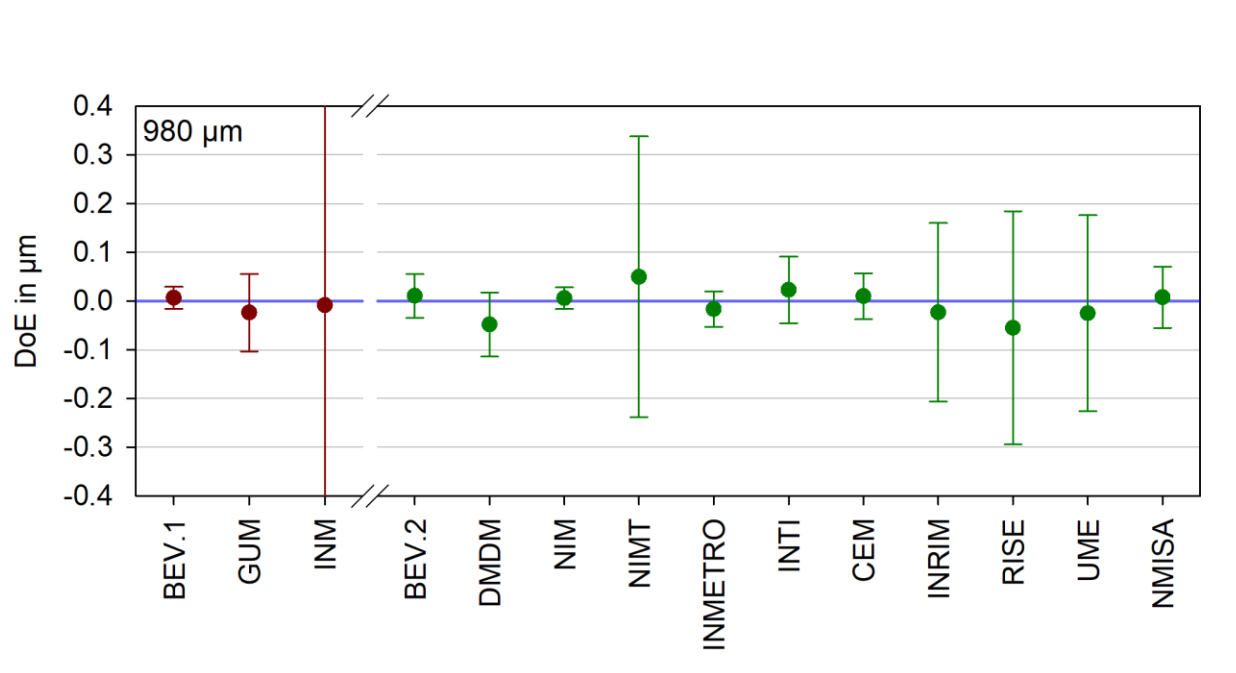


Figure 25 Degree of equivalence (d_{98}) of all participants for the line mark 980 μm . The error bars denote the expanded measurement uncertainty $U(d_{98})$ for $k = 2$. Red symbols (left to axis break) for results of participants of loop 1, green symbols (right to axis break) for results of participants of loop 2. Error bars for INM are too large for the chosen scale.

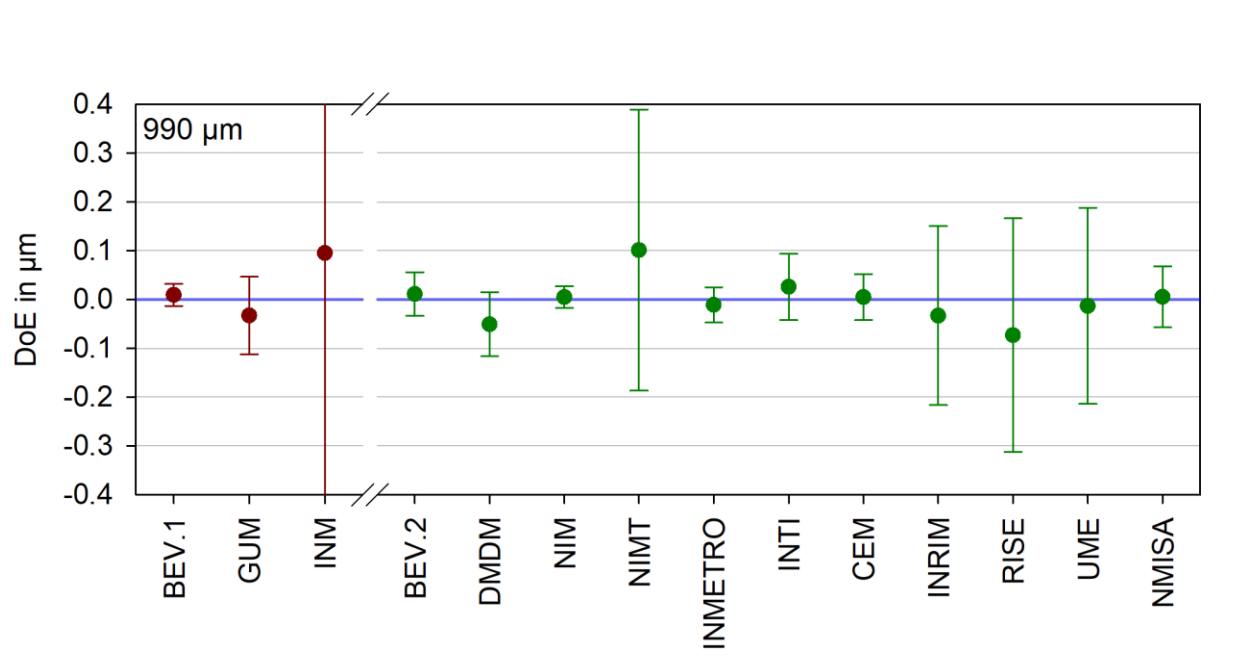


Figure 26 Degree of equivalence (d_{99}) of all participants for the line mark 990 μm . The error bars denote the expanded measurement uncertainty $U(d_{99})$ for $k = 2$. Red symbols (left to axis break) for results of participants of loop 1, green symbols (right to axis break) for results of participants of loop 2. Error bars for INM are too large for the chosen scale.

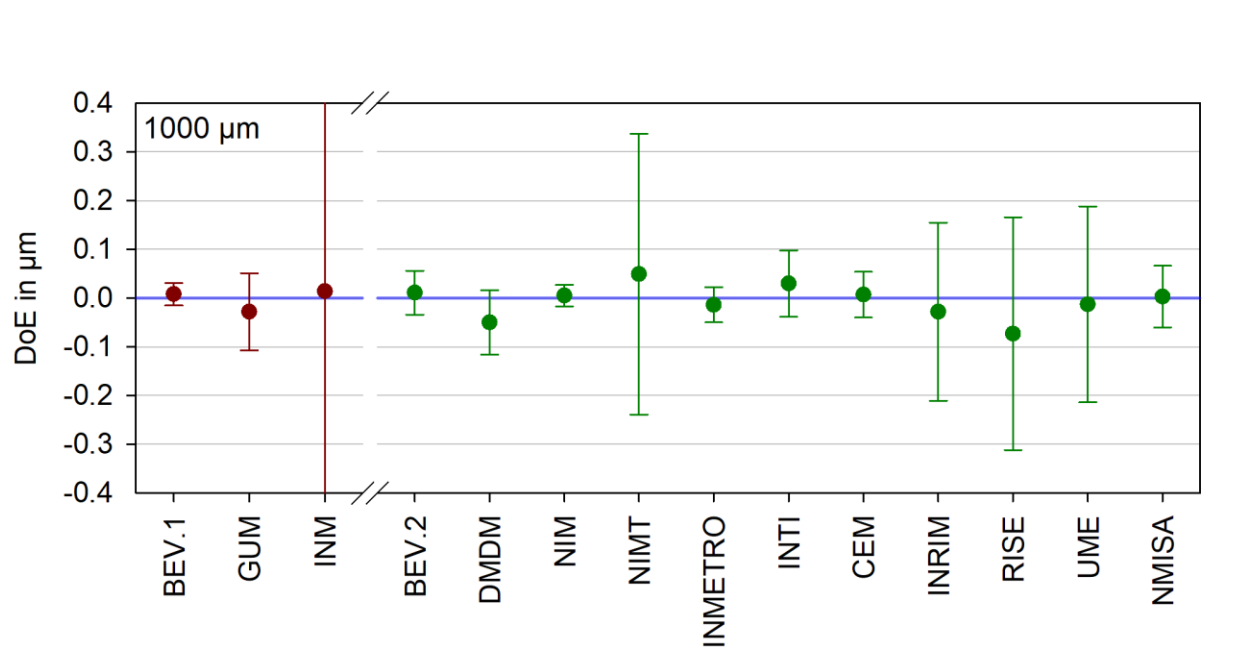


Figure 27 Degree of equivalence (d_{100}) of all participants for the line mark $1000 \mu\text{m}$. The error bars denote the expanded measurement uncertainty $U(d_{100})$ for $k = 2$. Red symbols (left to axis break) for results of participants of loop 1, green symbols (right to axis break) for results of participants of loop 2. Error bars for INM are too large for the chosen scale.

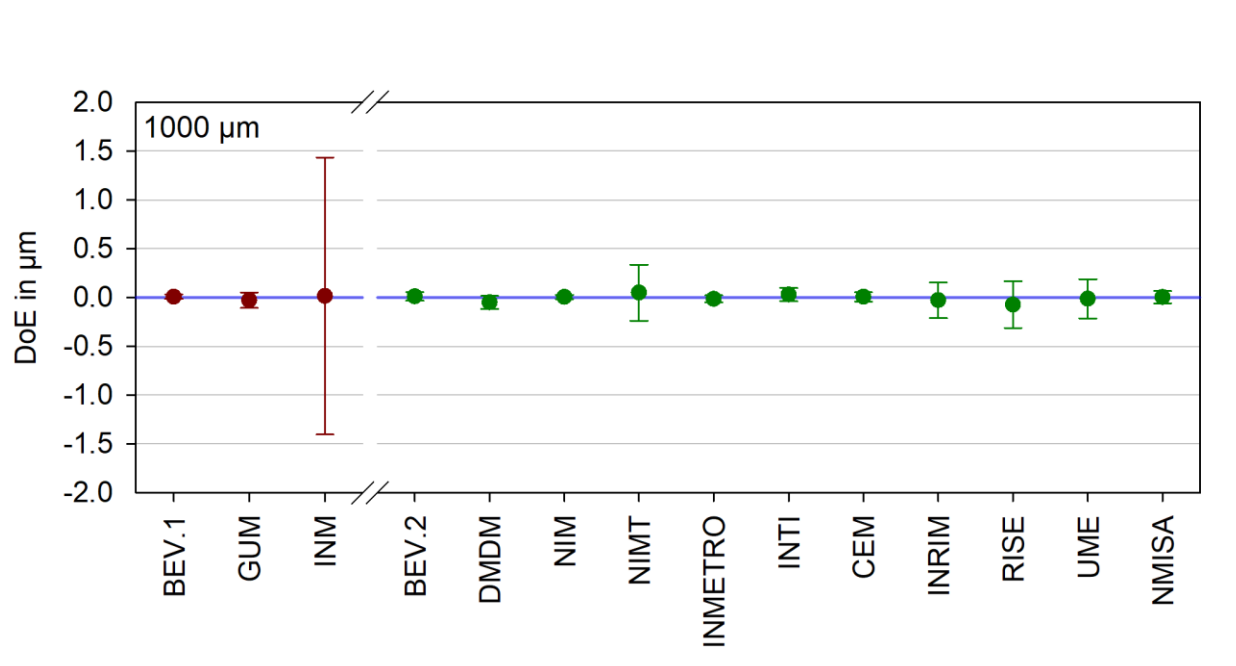


Figure 28 Degree of equivalence (d_{100}) of all participants for the line mark $1000 \mu\text{m}$. Same data as of **Figure 27** with expanded ordinate scale to visualize INM value.

6.5.3 Tabular representation of normalized DoE results (E_n)

Table 9 summarizes the E_n values of all participants for both loops. The are rounded to two decimal figures.

- All E_n values were smaller than 1 already from the pre-draft A state on. No separate analysis of a largest consistent subset was necessary therefore. (Table 9)
- With the exception of one participant (INM), the expanded measurement uncertainty for this service covered the range of 28 nm up to 290 nm (span of approximately 1:10). The uncertainties are plausible and adequate for this service category.
- However, one participant (INM) stated a very high expanded measurement uncertainty of up to 1420 nm. This is also twice as large than their published CMC value.
- The first loop with only three participants (BEV, GUM, INM) is effectively numerically equivalent to a bilateral comparison since one participant stated very high uncertainties.
- No link between the two loops was performed. BEV is the only participant common to both loops.
- From the statistical point of view (which might not be adequate) it is tempting to assume that the participants somehow overestimate some uncertainty contributions (1400 values without a single outlier).
- All published CMCs (with the exception of INM) are confirmed or even outperformed (see section 6.6.1).

6.6.1 Reported and published measurement uncertainties

The participants were asked to state the expanded measurement uncertainties for this comparison as well as published CMCs for this service. Table 10 summarizes this data. All values have been converted to nanometres. The expanded uncertainty is parametrized by the two constants a and b as in the following equation:

$$U = Q[a, b \cdot L] \equiv \sqrt{a^2 + (b \cdot L)^2}$$

Table 10 Stated and published expanded measurement uncertainties for participants of this comparison

| NMI | This comp | | CMC | | Comment |
|---------|-----------|-----------|--------|----------|--|
| | a | b | a | b | |
| BEV | 48 nm | 0 | 400 nm | 0 | |
| GUM | 90 nm | 0 | 268 nm | 0 | |
| INM | 1000 nm | 0.0005 | 500 nm | 0.0005 | Reported uncertainty much higher than CMC. Stated uncertainty equation not compliant with reported results. See INM comment below. |
| DMDM | 68 nm | 0.38E-06 | — | — | |
| NIM | 28 nm | 0.16E-06 | 104 nm | 0.16E-06 | |
| NIMT | 288 nm | 0.487E-06 | — | — | |
| INMETRO | 40 nm | 0.443E-06 | — | — | |
| INTI | 70 nm | 0.01 | — | — | |
| CEM | 50 nm | 0.25E-06 | 60 nm | 0.30E-06 | |
| INRIM | 90 nm | 2.0E-06 | 90 nm | 5.0E-06 | |
| RISE | 240 nm | 22E-06 | 500 nm | 0.5E-06 | |
| UME | 200 nm | 2.6E-06 | — | — | |
| NMISA | 65 nm | 0.001 | 250 nm | 0.001 | |

INM commented its reported results after circulation of the draft A report:

“The artefact was suspected to be damaged, before we realized and we reported the found values of the measurements. The microphotography of the artefact, that clearly were presented in Figure 8, 9, 10 and 11 from Draft B.0 of the Report, are confirming our presumption.

The reported values were influenced by the asymmetric deformation of the stage micrometer lines and the resulted and calculated uncertainty had to be increased.

Next step will be to participate in bilateral comparison and reinstate, at least, the current CMC uncertainty.”

6.7 Linking of result to other comparisons

The CIPM does not require to link supplementary comparisons. No link was performed therefore.

7 Equipment and measuring processes of the participants

Despite the seemingly standardized artefact, a wide range of equipment or techniques has been used. The participants have been asked to supply this information verbatim in a format ready for inclusion.

7.1 BEV

For the calibration of stage micrometers BEV uses the Nanopositioning and Nanomeasuring Machine NMM-1 (SIOS GmbH) with a laser focus sensor as the probing element. The NMM provides a measuring range of 25 mm × 25 mm × 4 mm, controlled by three orthogonally laser interferometers. The axes of three interferometers intersect virtually at the point of the probing element thus providing Abbe-free length measurements in all three coordinates. In this procedure the laser focus sensor is used to keep the surface of the stage micrometer in this point. The stage is moved in z-direction while scanning in the x- and y-directions. Beside the height information (which is not used in this application) the LFS provides also reflectivity values of the surface. The reflectivity is used for the line detection.

A rectangular field, which includes the ROI, of the sample is scanned and the reflectivity with its (x, y) coordinates is recorded. Usually a point spacing of 10 nm or 20 nm and a profile number of around 50 was used for the reported results. Both scan directions (regarding to the profiles) are recorded and evaluated. The duration of a typical scan is about 2 hours and produces files of up to 4 GB. The files are text files of a proprietary format.

The sample temperature is measured with a Pt100 sensor near the stage micrometer. Due to the construction principle of the machine the sample temperature deviates significantly from the air temperature of the laboratory.

Traceability route

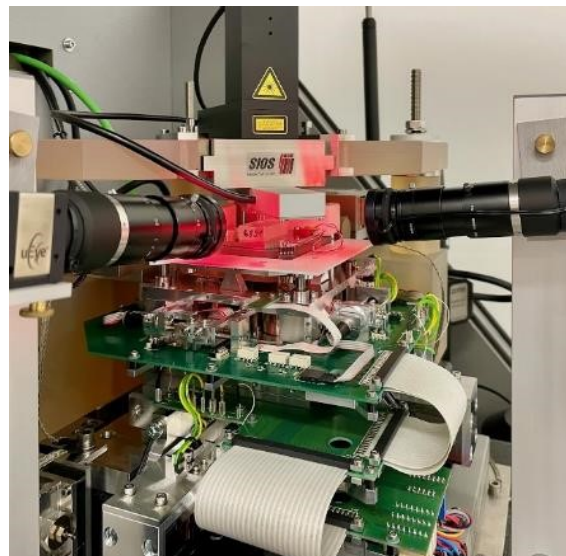
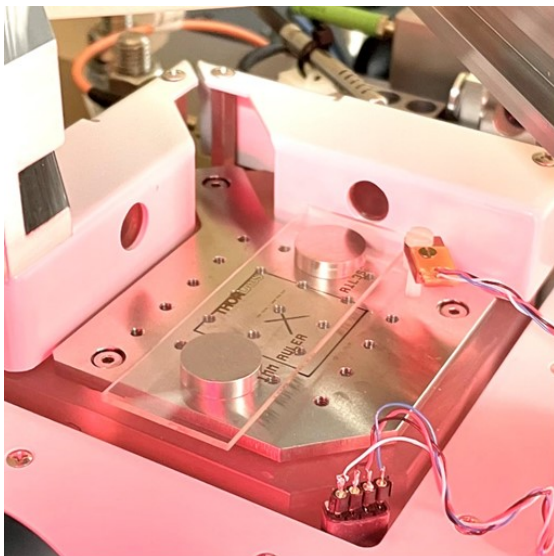
Traceability is guaranteed by the laser interferometers of the NMM. The three sources are calibrated by beat measurement with an iodine stabilized HeNe-laser. The environmental sensors are calibrated in house also.

Principle of line center detection

The scan data files are analysed using a homemade software. The evaluation is performed for each profile separately. The reflectivity data is segmented using a threshold to detect edges eventually after applying morphological filters. Line center is defined as the mid-point of two edges with opposite orientation. The evaluation procedure delivers also quality parameters like line width variation and edge roughness. The algorithm is documented in <https://github.com/matusm/NmmStageMicro>

Temperature range during measurements

20,9 °C to 22,8 °C (sample temperature)

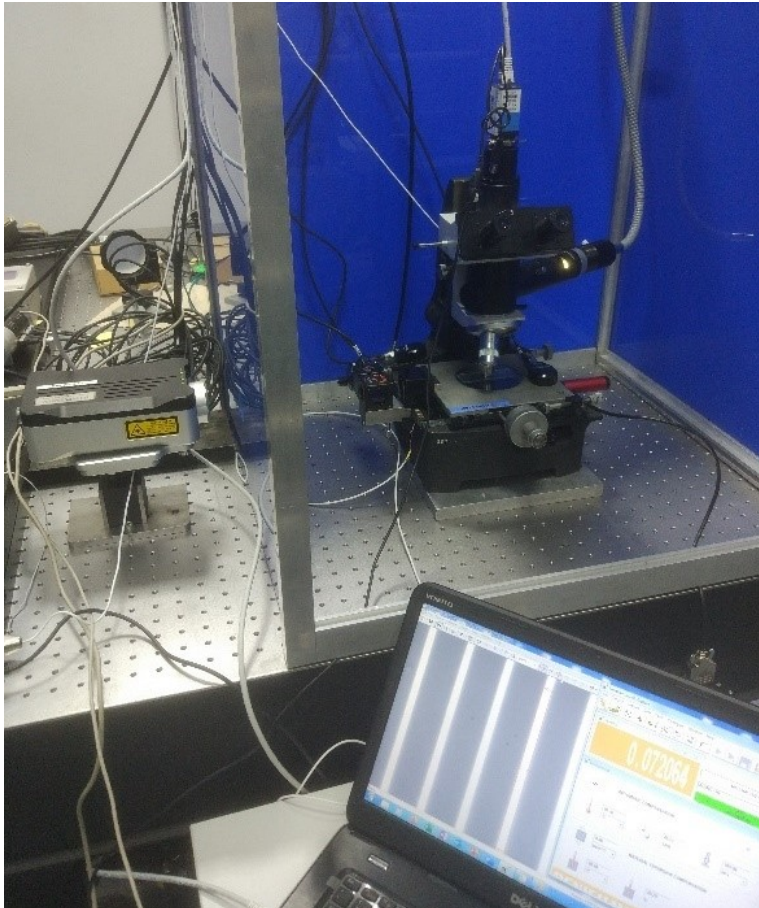


7.2 GUM

The stage micrometer was measured on the upgraded measuring microscope (Epi-illumination type in comparison) with CCD-camera.

The line spacing is measured with the laser interferometer Renishaw XL-80.

The stage is moved by piezoelectric actuators and high-resolution stepper motor, placed opposite each other.



Traceability route

Laser interferometer (Renishaw XL-80)

Principle of line center detection

The lines were positioned symmetrical in the 50 μm height ROI window and a width adjusted to the width of the graduation lines. The scale lines are aligned in ROI by eye in a symmetrical manner with precision piezo-electric actuator.

Temperature range during measurements

20,00 $^{\circ}\text{C}$ to 20.50 $^{\circ}\text{C}$ (for all measurements);

Temperature variation during a series of 3 measurements: 0,10 $^{\circ}\text{C}$

Additional remarks

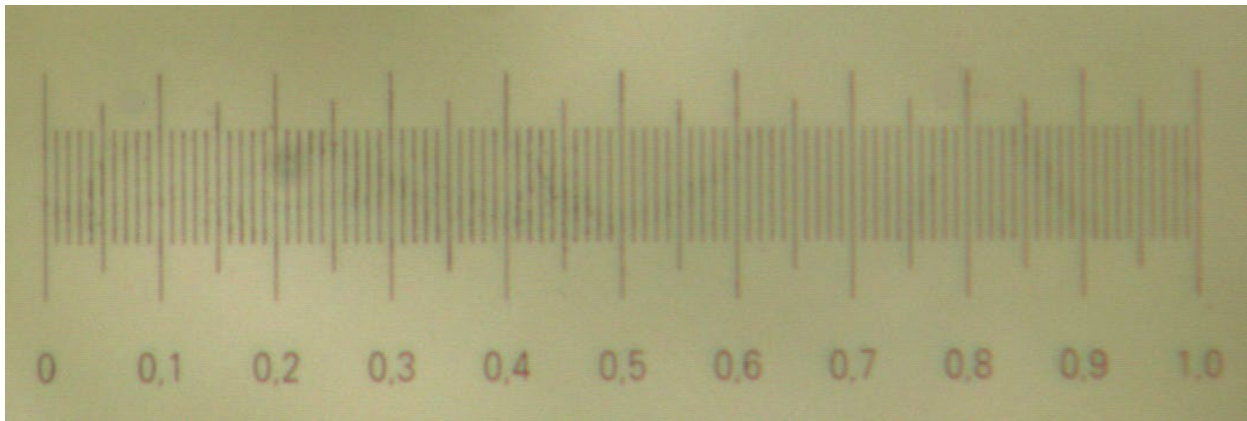
24 series (3 \times 8) of measurements were made, separately every 0.01 mm and separately every 0.02 mm. Due to small negative linear thermal expansion coefficient ($(-0.1 \pm 0.7) \cdot 10^{-6} \text{ K}^{-1}$), its value has been included only in the measurement uncertainty.

7.3 INM

Instrument: measurement length machine, equipped with an optical microscope and CCD camera.

The longitudinal comparator is based on the cinematic method, according to Abbe principle: the line scale of the stage micrometer must be aligned on the same longitudinal axis with measurement direction, in the scope to eliminate the first order errors. Because the line scale was very short, it was supported with the whole surface on the special carriage of the comparator and the scale was illuminated from bottom.

The standard used for the calibration of the length measuring machine is a laser interferometer used in current calibration services offered by INM.



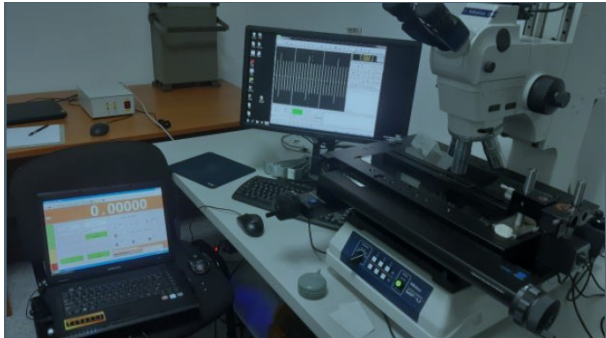
Method of measurement consists in the displacement of the scale along the measurement direction. During one measurement between the beginning and the end of the measurement, difference between the thermometer readings was equal to $\Delta t_g = 0.01 \text{ }^\circ\text{C}$

The difference between the temperature of the room and the reference temperature was $0.1 \text{ }^\circ\text{C} \dots 0.2 \text{ }^\circ\text{C}$ during all measurements.

7.4 DMDM

Positioning system: CCD measuring microscope Mitutoyo MF-UB3017C (3 axes type), glass measuring stage (300x170) mm, LED illumination, reflected light, objective Mitutoyo M Plan Apochromat 50X magnification NA 0.55, total magnification: 500X optical, 4X digital, CCD camera Mitutoyo Vision unit 3.0 MP, commercial software Mitutoyo QSPAK Vue ver.4.0

Measuring system: Laser interferometer Renishaw XL80, Renishaw measuring sensors for air and material temperature, air pressure and relative humidity, commercial Renishaw software for linear (distance) measurement.



Traceability route

Laser interferometer

Principle of line center detection

Visually, using CCD camera, Mitutoyo software and different types of crosshairs. There is no special software dedicated for line center detection. Measuring stage with stage micrometer was moving manually and microscope objective was fixed during measurements.

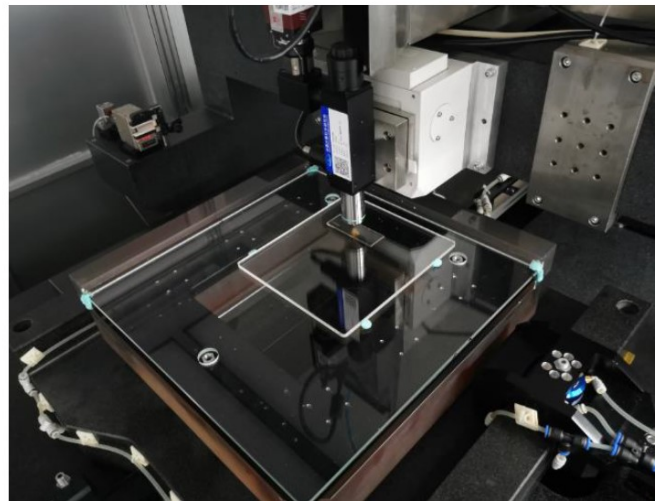
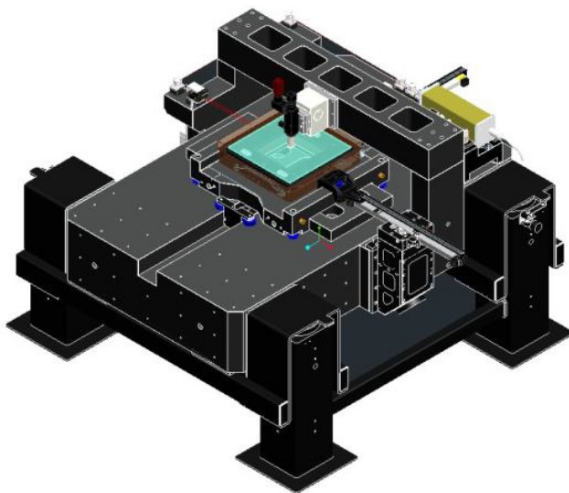
Temperature range during measurements

19.50 °C to 20.50 °C

7.5 NIM

The results of this comparison are obtained by the high precision two-dimensional measuring instrument with laser system. The two-dimensional measuring instrument with laser system was established with the techniques of laser interferometry and image aiming. It is a non-contact 2D coordinates measuring system with laser interferometer as length measuring standard, imaging with CCD and microscopy, auto measuring with computer image processing and error compensating techniques. The measuring range of the instrument is 300 mm × 300 mm, which can reach to 500 mm in a single direction by splicing measurement.

The coaxial reflected light is used for illumination in this comparison.



Traceability route

The laser interferometer uses a frequency-stabilized laser as the measuring light source, and the laser wavelength is traced to the national 633nm wavelength standard.

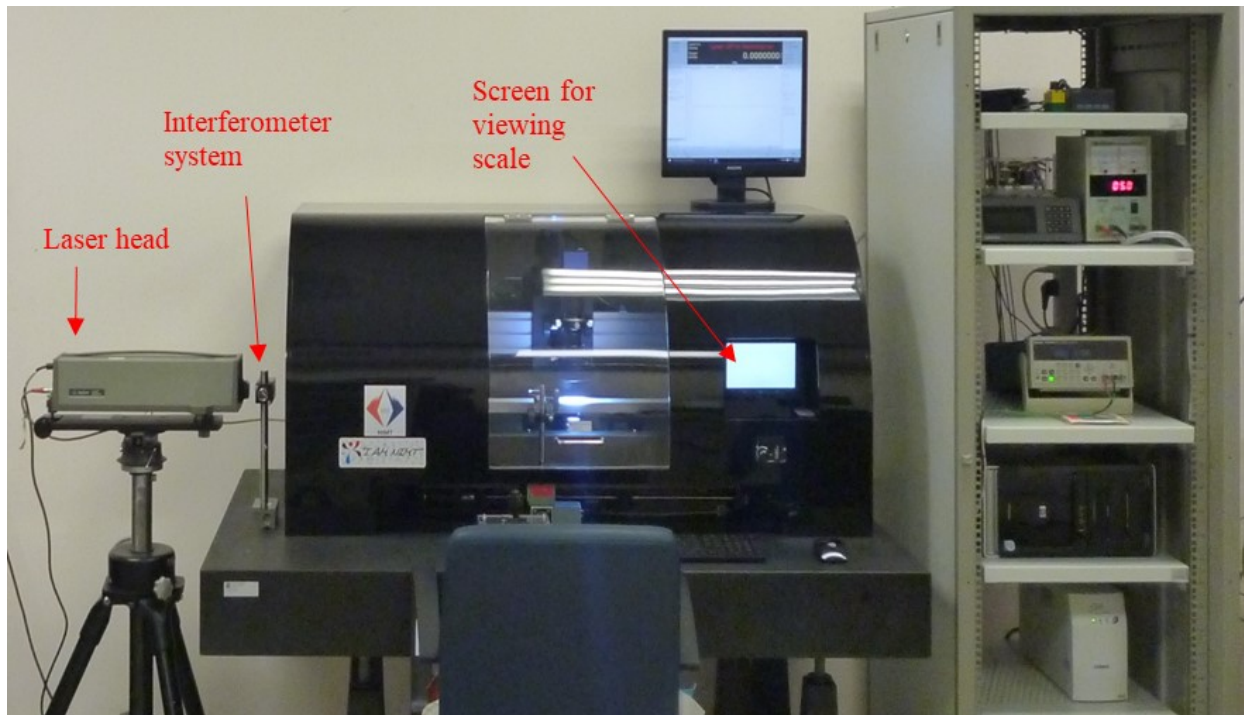
Principle of line center detection

During measurements, the optical imaging system is fixed, the micrometer moves with the working platform, and its line is aimed with the optical imaging system. The line space is the sum of the displacement of the movement platform measured by the laser interferometer and that of the line measured by the optical imaging system. The center of the line is calculated by parallel line fitting algorithm.

Temperature range during measurements

19.95 °C to 20.05 °C

7.6 NIMT



Traceability route

The wavelength of Laser Interferometer was calibrated using Iodine stabilized He-Ne laser by beat frequency method.

Principle of line center detection

We measure the left side of the line of scale and measure the right side of the line of scale to find the center line.

Temperature range during measurements

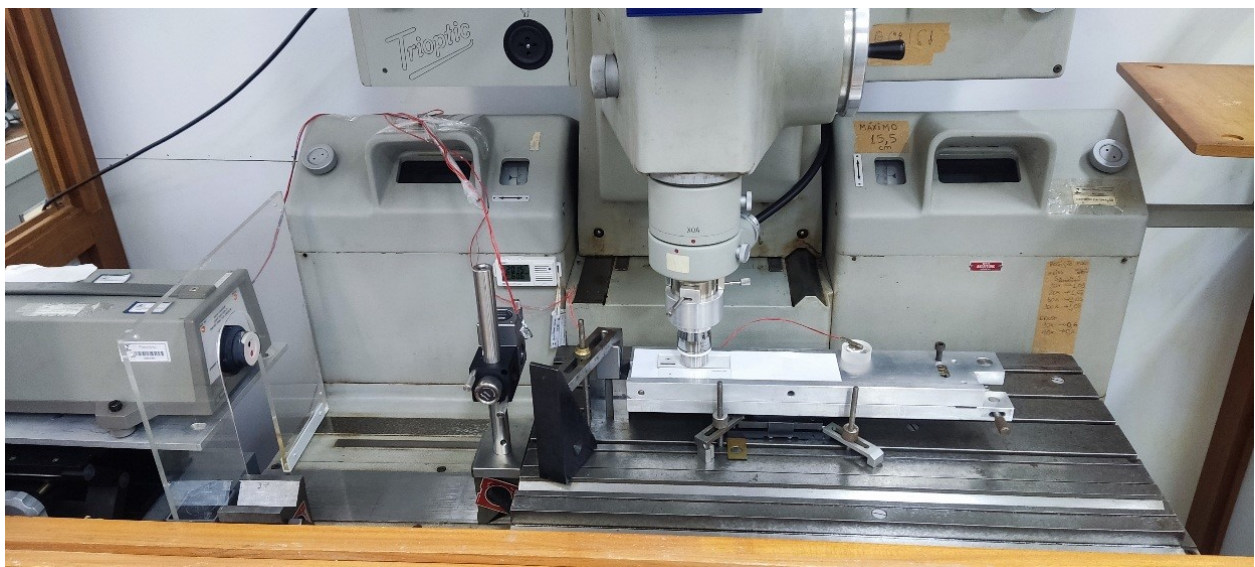
19.52 °C to 19.74 °C

7.7 INMETRO

Inmetro's linescales measurement system is composed by a laser system, SIP-Trioptic measure machine, vision system and reflected illumination. A special alignment and levelling table are mounted over the machine table. The special table has screws which rotates the table in two different angles that allows the rotation of artifact in pitch and yaw. The artifact is placed on the special table and a lens set with a CCD camera acquires images of the artifact.

For levelling, the artifact is moved together with the table of measure machine in scale direction and the pitch movement is adjusted to ensure the focus in the full scale at a certain magnification. For alignment, the table is also moved in the scale direction and in this case, the bottom of the first and the last scale lines are considered to adjust scale position and make sure that it remains at same image pixel position. The yaw rotation is used for that. In some cases, that is not the present one, the artifact has alignment structures that may be used to align it.

A laser system is aligned with measure machine table movement and gives traceability to the measurement system combined with pixels counting of snapped images. The pixel calibration is made each running by two images of the same line. The center pixel position is obtained computationally in different positions and it is correlated with the laser display at that position. These values allow estimation of the real recomposed line position.



The distances are obtained by the difference between the line of interest and the reference line (zero point). The region of interest (ROI) of the images is mainly took at middle of lines. The highest magnification of the system disposes an image region around 60 μm height and a pixel size of 60 nm. The system allows measurements range up to 300 mm unidirectional standards.

It is also possible to measure bidimensional gages using this system although the limit for this other direction is about 150 mm. For that, another table is attached to the special table. The procedure for levelling is the same of the previous one but, in this case, the table stays still and the lens set moves.

An additional levelling is needed in this case to rotate the artifact in roll. On other bidirectional artifact direction.

Traceability route

The traceability is provided by a laser interferometer system. The pixels are calibrated each running by the snapping of two image and the correlated laser positions. The final center line position is composed of these laser and center pixel lines positions. Measurements are compensated using reference conditions

described below at additional remarks. For that, calibrated temperature, air pressure and humidity sensors are used to monitor these variables throughout the calibration.

Principle of line center detection

The line center detector starts with a Kirsch edge detector (a convolution matrix is applied to the image matrix using eight different directions to find the highest intensity directional edge). The found points are weighted to transform them in subpixel edges points. The first edge fit is performed at each edge. For noise attenuation, the error between edge points and first fits is used considering an interval from median point to reduce the influence of probable noise points. A second edge fits is performed and the center position of the line is calculated by average value of edges second fits middle positions.

Temperature range during measurements

Air: 19.858 °C to 20.174 °C

Standard: 19.877 °C to 20.041 °C

Additional remarks

Reference conditions for reported results:

Air temperature: 20 °C

Standard temperature: 20 °C

Air pressure: 760 mmHg

Relative humidity: 50 %

CO2 concentration: 0.04 %

Uncertainty budget

| Input Quantity x_i | Distrib. | $U(x_i)$ unit | v_i | $c_i = \partial dL / \partial x_i$ | $u_i(dL) / nm$ |
|----------------------|----------|---------------|-------|------------------------------------|----------------|
| Repeatability | N | 5 nm | 19 | 1 | 5 |
| Resolution | R | 1 nm | 100 | 1 | 0.3 |
| Laser instability | R | 3 nm | 50 | 1 | 2 |
| Laser alignment | R | 6 nm | 50 | 1 | 3 |
| Deadpath | R | 25 nm | 50 | 1 | 14 |
| Abbe error XZ | R | 4 nm | 50 | 1 | 3 |
| Abbe error XY | R | 1 nm | 50 | 1 | 0.5 |
| Pixel size | R | 15 nm | 100 | 1 | 9 |
| Center deviation | R | 12 nm | 50 | 1 | 7 |
| Air temperature | R | 0.03 °C | 50 | 1.63E-8 (1/°C) | 0.02 |
| Atm. Pressure | R | 49 Pa | 100 | 2.7E-9 (1/Pa) | 0.08 |
| Humidity | N | 18 Pa | 100 | 3.7E-10 (1/Pa) | 0.004 |
| Standard Temp. | N | 0.01 °C | 50 | 1E-7 (1/°C) | 0.0006 |
| Wavelength | N | 3 pm | 100 | 1.3E-5 (1/mm) | 0.00002 |
| Horizontal alignment | R | 0.6 mrad | 50 | 6E-4 (1/rad) | 0.2 |
| Vertical alignment | R | 0.05 mrad | 50 | 5E-5 (1/rad) | 0.002 |
| Expansion coef. | R | 0.7E-7 (1/°C) | 100 | 131 °C | 0.005 |

Combined standard uncertainty:

$$u_i(dL) = 20 \text{ nm};$$

Effective degree of freedom:

$$v_{eff}(dL) = \infty;$$

Expanded uncertainty:

$$U_{95}(dL) = Q[40 \text{ nm}, 443E^{-9} L];$$

7.8 INTI

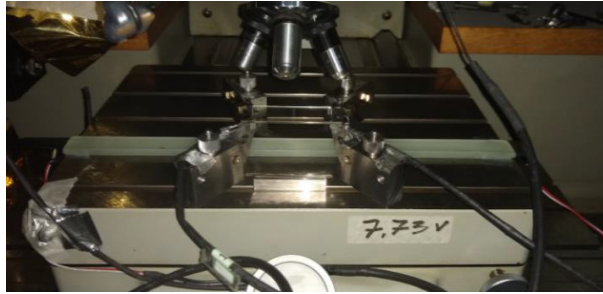
CMM SIP, model 420-M.

Laser HP, model 5529A.

Fixed microscope Zeiss with Basler CCD camera

Thermometer Cole Palmer, model 08502-16.

Illumination type: LED white light



Traceability route

Laser interferometer HP, model 5529A calibrated by beat frequency with reference laser He-Ne of INTI.

Principle of line center detection

A microscope with a camera and in-house software for the line detection was used.

Temperature range during measurements

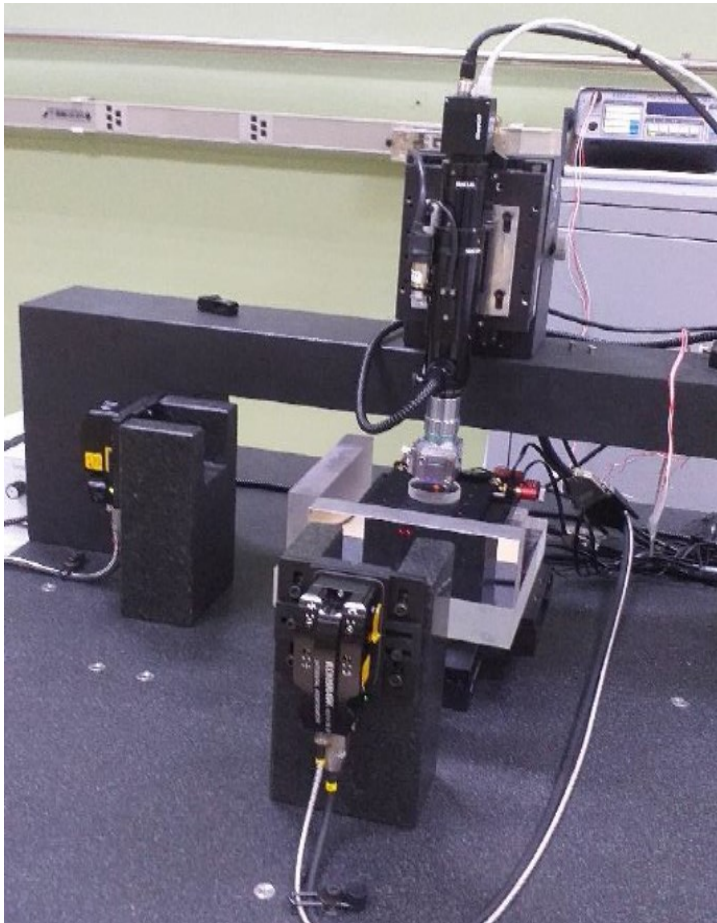
The temperature range of the room is $(20.0 \pm 0.5) ^\circ\text{C}$. The change of the gauge temperature during measurement was less than $0.1 ^\circ\text{C}$

7.9 CEM

The distances between graduation lines were measured with a 2D measuring system with 110 mm x 110 mm range. The system consists in a high accuracy XY stage with a Zerodur® block with two perpendicular mirrors attached. On top of the block there is a motorized six-DoF table used for fine alignment. The system is completed by an additional Z-axis that holds a high-quality optical objective, a motorized zoom and a CCD camera. Two reference mirrors are attached to the objective.

Movement of both axes is measured by a differential interferometric system made up of two stabilized Renishaw RLU20 laser encoders and two differential RLD10-DI detectors. Air temperature, pressure and humidity were measured to determine the refraction index of the air by Edlen formula.

The graduations lines are localised by means of a microscope with a CCD camera and an episcopic coaxial illumination system. In each measurement, the graduation line is aligned with the centre of the field of view of the microscope while the reading of the interferometer is captured. The relative position is determined by digital image analysis with subpixel accuracy.



Traceability route

Laser interferometer calibrated against the length national standard.

Principle of line center detection

The line scale was aligned parallel to X-axis of the 2D measuring system. Each vertical graduation line is analysed within the ROI of 50 μm width around the center line position. The center of the line profile is the average of the left and right edges. The edge locations are determined by the Best Projection method, finding the strongest projected edge location to determine the straight edge, using the vision library of National Instruments.

Temperature range during measurements
20.05 °C to 20.34 °C

Additional remarks
Uncertainty Budget

Stage micrometer

Id cal/comp :

| | |
|-----------------------|----------------------|
| Description artefact: | |
| Description: | 1 mm |
| Manufacturer: | Präzisionsoptik Gera |
| Serial number: | BEV |
| Substrate material: | Nextrema ® 724-3A |

| | | |
|----------------------|-------|-------|
| Translation stage: | | |
| | units | value |
| Id traslation stage: | | |
| Yaw of y-axis: | " | 12 |
| Pitch of y-axis: | " | 12 |
| Abbe offset y: | mm | 0,5 |
| Abbe offset z: | mm | 0,5 |

| | | |
|---|-------|----------|
| Interferometer: | | |
| | units | value |
| Vacuum wavelenth value: | nm | 632,99 |
| Vacuum wavelenth uncertainty: | rel. | 1,0E-08 |
| Eddien equation: | rel. | 1,0E-08 |
| Air temperature uncertainty: | °C | 0,05 |
| Air pressure uncertainty: | Pa | 35 |
| Air humidity uncertainty: | Pa | 48 |
| Drift temperature (during measurement): | °C | 0,3 |
| Drift pressure (during measurement): | Pa | 10 |
| Drift humidity (during measurement): | Pa | 10 |
| Interferometer deadpath: | mm | 20 |
| Optics nonlinearity: | nm | 2,2 |
| Optics thermal drift: | nm | 4 |
| cosine error (laser missalignment) | nm | 5,00E-09 |

| | | |
|--|------------------|----------|
| Stage properties: | | |
| | units | value |
| Stage alignment horiz.: | µm/mm | 0,05 |
| Stage alignment vert.: | µrad | 100 |
| Line definition: | nm | 10 |
| Temperature deviation between calibration: | °C | 0,05 |
| Thermal exp. coef.: | °C ⁻¹ | -1,0E-07 |
| Uncertainty exp. coef.: | °C ⁻¹ | 7,0E-07 |
| Drift temp along measurement | °C | 0,3 |

| | | |
|--|----------|-------|
| Image processing | | |
| | units | value |
| Microscope magnification deviation axis: | nm/pixel | 70 |
| | pixel | 0,001 |
| Influence of line edge detection algorithm | nm | 14 |

| | | |
|-----------------|-------|-------|
| Measurement: | | |
| | units | value |
| Repeatability: | µm | 0,05 |
| N° of measures: | | 30 |

| | | |
|---------|----|---|
| Length: | | |
| | mm | 1 |

| Input quantity x _i | Symbol | Value | Units | Probability distribution | uncertainties | | degrees of freedom, v | | sensitivity coefficient c _i | sensitivity coefficient value | uncertainty contribution to u(L) | degrees of freedom v | relative weight (in %) |
|---|------------------------------|---------------------------|-------|--------------------------|--------------------------|----------------------------------|-----------------------|-------|--|-------------------------------|----------------------------------|----------------------|------------------------|
| | | | | | u(x _i) | u _c (x _i) | partial | total | | | | | |
| Interferometer | | | | | | | | | | | | | |
| Vacuum wavelenth | λ ₀ | 632,990 nm | | normal (k=2) | | 2,4E-09 | 100 | | 100 | δ(λ ₀)=nm/nm=L | 1 | 100 | 2,5E-07 |
| Index of refraction (calculation) | | | | | | | | | | | | | |
| temperature measurement | t | | | | | 0,09 °C | 116 | | δ(t) | 8,56E-07 | | 188 | 1,5E-03 |
| thermometer measurement uncertainty | cal _t | 0,05 °C | | normal (k=2) | 0,025 °C | | 100 | | | | | | |
| drift temperature during measurement | Δt | 0,3 °C | | rectang. | 0,09 °C | | 100 | | | | | | |
| pressure measurement | p | | | | | 17,74 Pa | 100 | | δ(p) | 3,00E-09 | | | |
| sensor measurement uncertainty | cal _p | 35 Pa | | normal (k=2) | 17,5 Pa | | 100 | | | | | | |
| drift pressure during measurement | Δp | 10 Pa | | rectang. | 2,887 Pa | | 100 | | | | | | |
| humidity measurement | h _r | | | | | 24,17 Pa | 100 | | δ(h _r) | 3,63E-10 | | | |
| sensor measurement uncertainty | cal _{h_r} | 48 Pa | | normal (k=2) | 24 Pa | | 100 | | | | | | |
| drift humidity during measurement | Δh _r | 10 Pa | | rectang. | 2,89 Pa | | 100 | | | | | | |
| Eddien equation | n _{air} | 1,00E-08 (1) | | normal (k=1) | 1,0E-08 | | 100 | | 1 | 1 | | | |
| Dead path error | C _{DP} =DP·Δn (2) | 1,89 nm | | rectang. | 1,1 nm | | 100 | | 1 | 1 | 1,1 nm | 100 | 0,20 |
| Optics thermal drift | C _{SD} | 4,0 nm | | rectang. | 2,3 nm | | 100 | | 1 | 1 | 2,3 nm | 100 | 0,88 |
| Optics nonlinearity | C _{SN} | 2,2 nm | | rectang. | 1,3 nm | | 100 | | 1 | 1 | 1,3 nm | 100 | 0,27 |
| Cosine error (laser missalignment) | C _{CS} | 5,00E-09 L | | rectang. | 2,9E-09 L | 1,4E-09 L | 100 | | 1 | 1 | 1,44E-09 L | 100 | 3,5E-07 |
| Translation stage | | | | | | | | | | | | | |
| Errors due to Abbe offsets and pitch and yaw of translation stage | Δ _{translation} | 41 nm | | rectang. | 11,9 nm | | 100 | | 1 | 1 | 11,9 nm | 100 | 23,37 |
| Stage properties | | | | | | | | | | | | | |
| Stage alignment horiz. | Δ _{hor} | 5,00E-05 rad | | rectang. | 1,2E-05 L | | 100 | | 1 | 1 | 1,2E-05 L | 100 | 2,6E-07 |
| Stage alignment vert. | Δ _{vert} | 1,00E-04 rad | | rectang. | 5,0E-05 L | | 100 | | 1 | 1 | 5,00E-05 L | 100 | 4,1E-06 |
| Line definition | Δ _{lin} | 10 nm | | rectang. | 2,9 nm | | 100 | | 1 | 1 | 2,9 nm | 100 | 1,38 |
| Thermal exp. coef. | α _L | -1,0E-07 °C ⁻¹ | | rectang. | 7,0E-07 °C ⁻¹ | | 100 | | Δ L | 0,092 L | 6,47E-08 L | 100 | 6,9E-04 |
| Temperature of stage | t _s | | | | | 0,092 °C | | | Δ t | -1,0E-07 L | -9,24E-09 L | 100 | 1,4E-05 |
| drift along the time | drift _t | 0,3 °C | | rectang. | 0,087 °C | | 100 | | | | | | |
| calibration sensor | t _{cal} | 0,05 °C | | normal (k=2) | 0,025 °C | | 100 | | | | | | |
| temperature deviation | Δt _{tem} | 0,05 °C | | rectang. | 0,020 °C | | 100 | | | | | | |
| reading | | | | | | | | | | | | | |
| repeatability | S _{rep} | 0,05 µm | | normal | 15,8 nm | | | | 1 | | 15,8 nm | 29 | 41,42 |
| Image processing | | | | | | | | | | | | | |
| microscope magnification (deviation of axis) | magn _{axis} | 0,1 nm | | normal | 0,1 nm | | | | 1 | | 0,1 nm | 100 | 0,00 |
| line edge detection algorithm | alg | 14 nm | | normal | 14,0 nm | | | | | | 14,0 nm | 100 | 32,48 |

(1) refs.: Metrologia, 1994, 31, 315-316 and Metrologia, 1998, 35, 133-139.
(2) Δn calculated for L=DP, taking into account Δp, ΔT and Δh_r variations as previously considered.

$$u_c = Q [a : bL] \quad a = 24,566 \quad b = 1,15E-07 \quad v_{(k=1 \text{ meas})} = 133$$

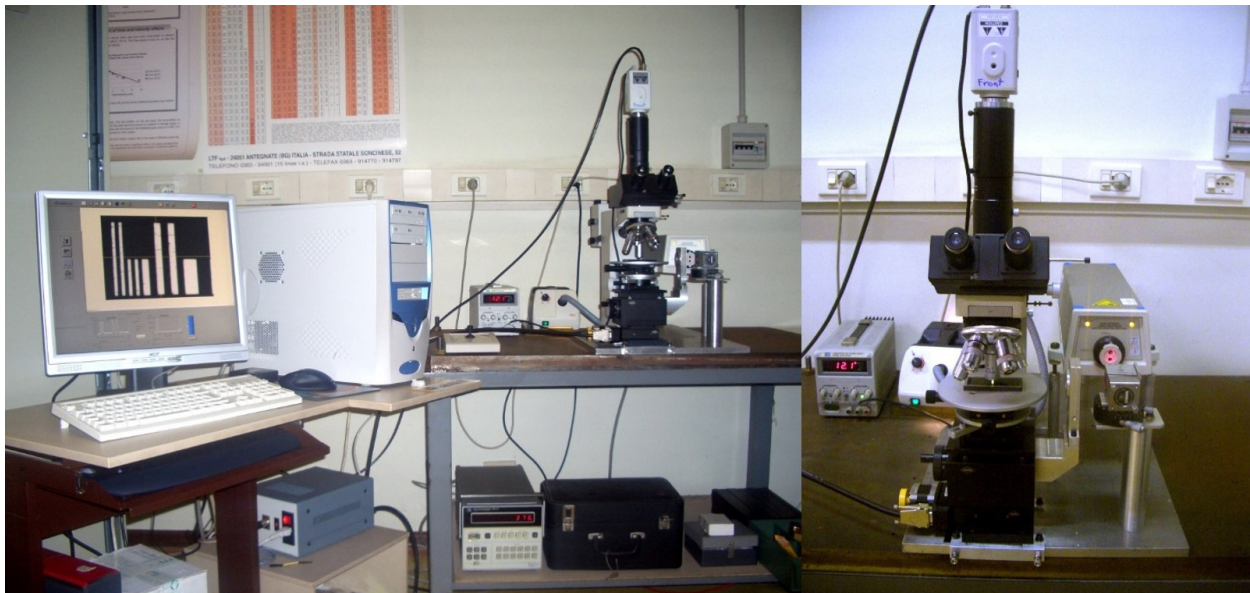
$$U (k=2) = Q [66 \text{ nm } 3,3 \times 10^{-2} L]$$

$$U (k=2) = 2 \cdot Q [25 \text{ nm } ; 1,2E-07 L]$$

7.10 INRIM

Measurement station consists essentially of:

- a metallographic microscope, equipped with:
 - 12 V – 100 W halogen illuminator, with a fine adjustment of framed field luminous intensity;
 - 5-position objective holder including flat-achromatic objectives 2,5X, 5X, 10X, 20X, 50X.
- a solid-state high sensitivity CCD;
- a multi cross-stage sample holder, with a configuration, as follows:
 - a special stage for allowing manual movements till to 15 mm along the z axis in order to keep the plane with the examined objects on the focus plane containing the optical path of the microscope and the axis of the probe. Practically, the user makes the right focus by this stage and not by the microscope coarse focusing that is blocked.
 - A motorized x-axis driven by the software.
 - A 360° rotary table.
 - A x/y manual motion by micrometric screw in order to center the field of view manually.
 - A circular plate for support of samples to be measured.
- HP laser interferometer composed of HP5518A head and HP5508A reader (wavelength 632991378 fm \pm 6 fm) perfectly aligned along motorized x-axis.
- Automatic measuring software (based on IMRiM patent).



Measurement procedure and principle of line center detection

The micrometer is positioned on a support plate adjustable transversally at 90° by means of two manual micrometric slides.

Manual slides are positioned on the upper plate of a vertical slide, which is also manual.

The support plate can rotate relative to the top plate of the vertical slide and the top plate of the slide can rotate relative to the vertical slide.

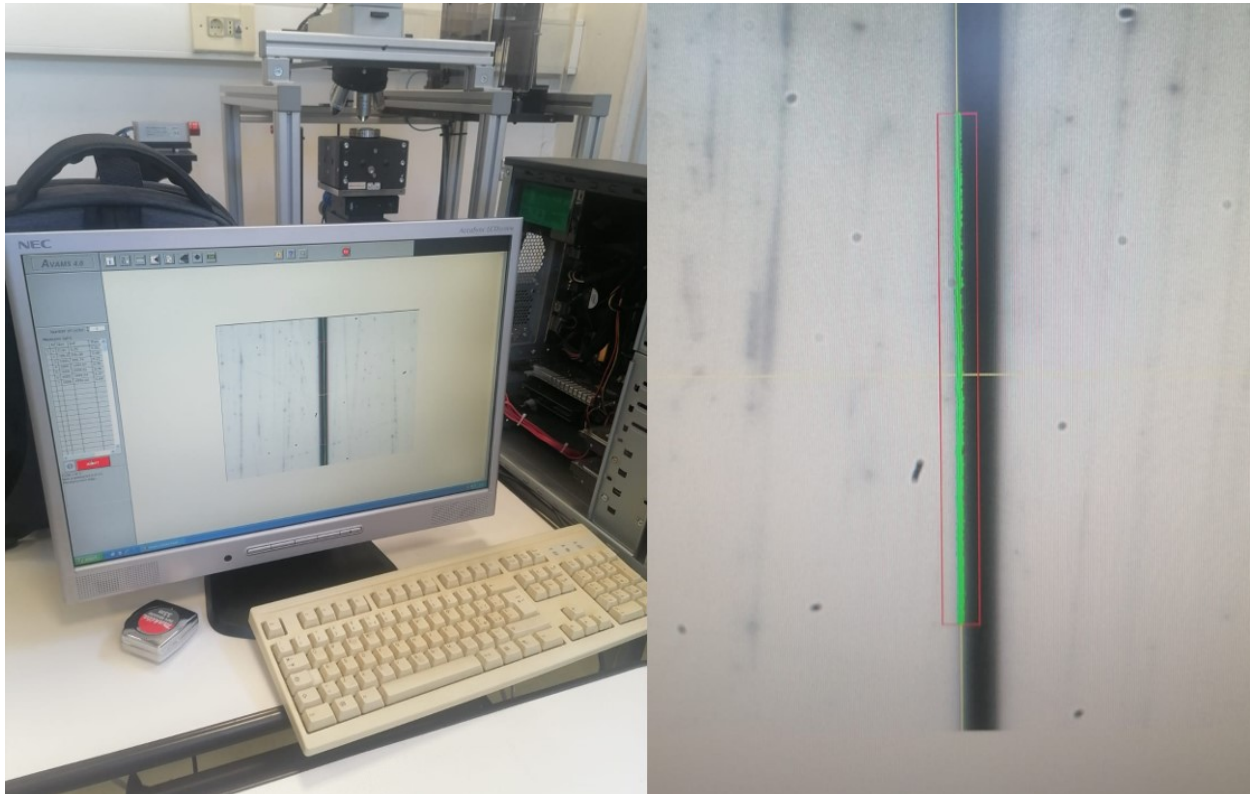
A motorized slide supports the system of manual slides and micrometer and carries out the movements.

The interferometric system, with a corner-cube integral with the mobile part of the motorized table, measures its movements by detecting the absolute position of the micrometer.

The various lines to be calibrated are brought inside the scanning window of the optical system by means of the motorized translation table.

A graphics processing program is used on the PC which, using a series of image analysis routines, reconstructs the profile of the features and determines their positioning within the scanning window.

Everything is controlled by the “Avams” software program operating on a PC.



Traceability route

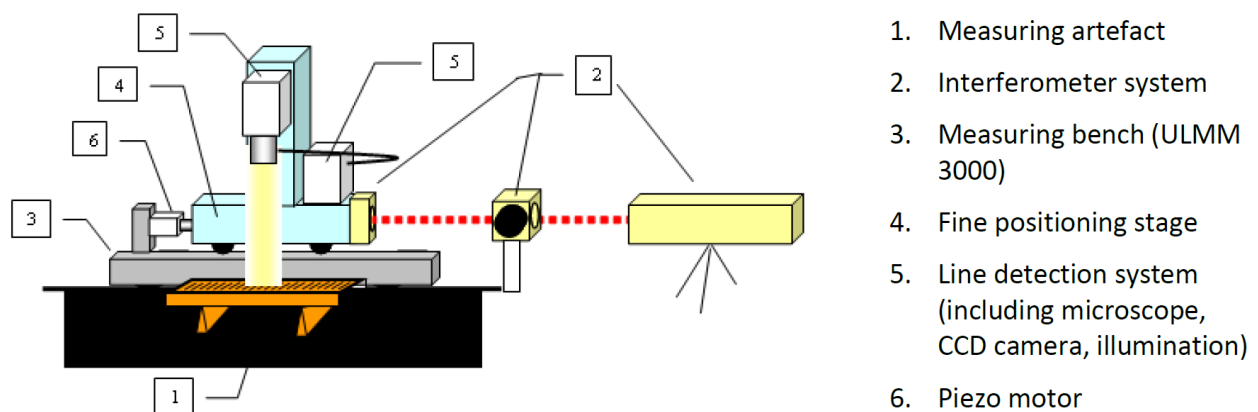
Laser interferometer (see above)

7.11 RISE

The system, presented in Figure 1, is in an underground laboratory with air temperature and humidity control. The temperature is 20 ± 0.2 °C and humidity 50 ± 5 % RH. All sensitive systems in the lab are standing on huge air-damped concrete blocks and the personnel has a separate floor, vibration isolated from the instrumentation, to use.

The measurement system is built up on a 1-D measuring bench (ULMM 3000) with a total measuring length of three meters. The scale is placed on mechanical supports of the bench with functionality for scale alignment. Flat support of the scale is used.

The translation stage of the bench consists of two parts. The main part is sliding (i.e. rolling) on a rail, used for manually moving it coarsely to the nominal positions of a line on a scale. The second part, mounted on the main part, is used for fine-tuning the translation. A microscope (Meiji MC-50, 20x lens) is mounted on this stage. A vision system is used in a closed loop with a piezo actuator (NPL NanoVision) for automatic fine tuning the microscope over the actual line.



Traceability route

A laser interferometer (Agilent 5519A System) is used for detecting the position of the lines. The retroreflector is mounted close to the microscope.

Principle of line center detection

NPL NanoVision sub-pixel accuracy length measurement system was used for line center detection. NPL NanoVision utilises digital analysis techniques to extract detailed edge and feature position information from images of the measured gratitudes. It works in combination with a piezo-electric stage pusher for fine motion control.

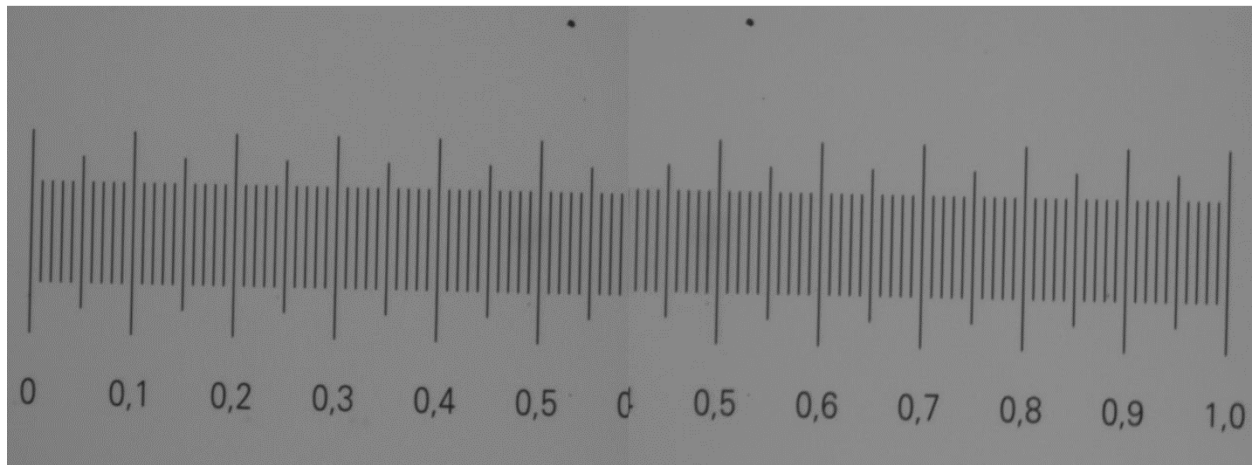
Temperature range during measurements

20.01 °C to 20.07 °C

The air- and material temperature of the scale (i.e scale support) are measured with an Isotech microK-800 system during the whole calibration process.

Additional remarks

Pictures after measurements, before departure, are shown below. There are dust particles on the glass around the scale, but we did not try to remove anything in case that would affect or damage the scale.



7.12 UME

The instrument used for the comparison is a 2D measuring instrument equipped with laser interferometer on its x and y axis. Air bearing x-y table moves on granite surface plate using nano-motors. Measurement is performed with front illuminated (reflected from sample) digital microscope with 50× objective with homemade software.



Traceability route

Traceability of measurement is provided with laser interferometer.

Principle of line center detection

Line center detection is done manually using home-made software.

Temperature range during measurements

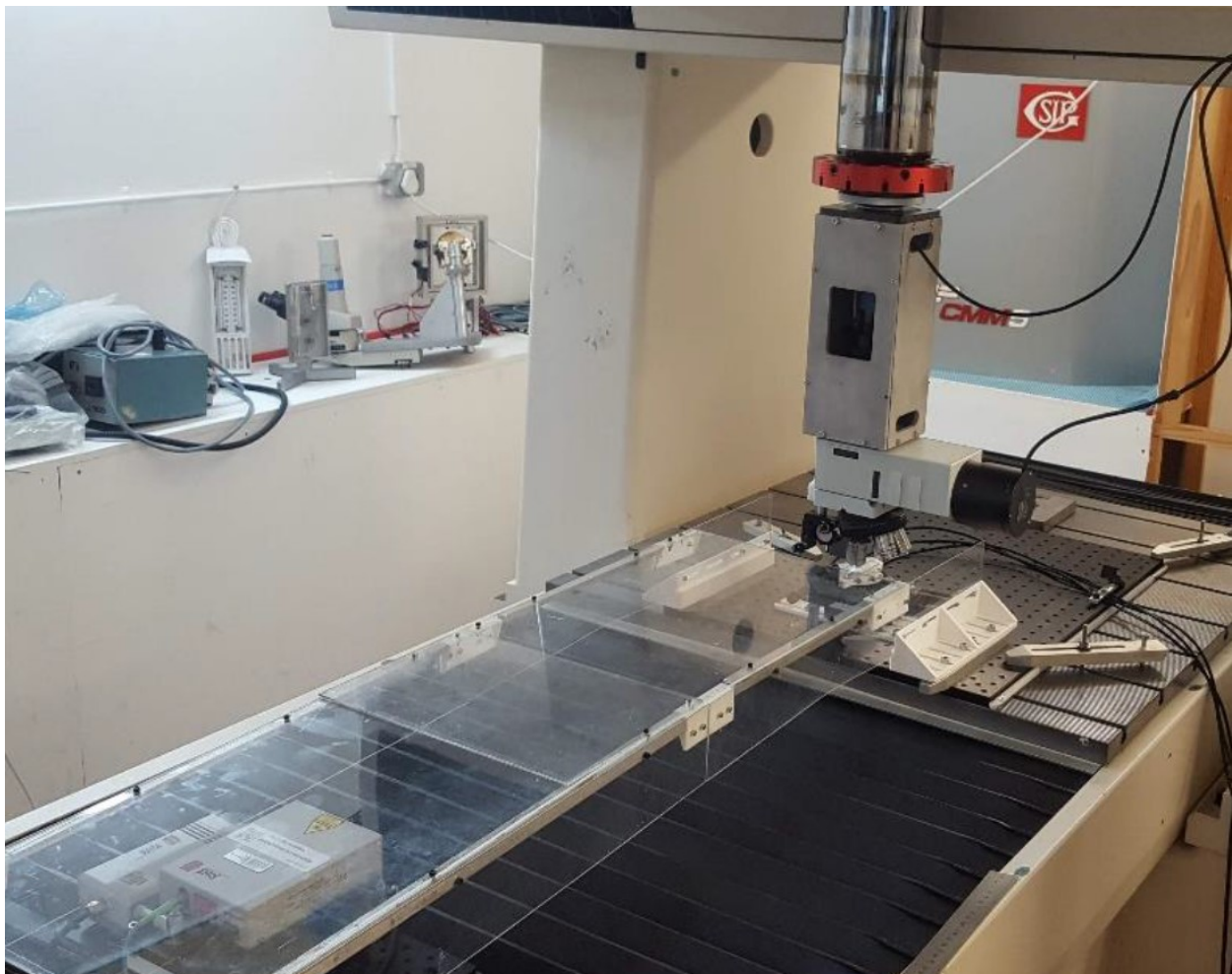
19.70 °C to 20,30 °C

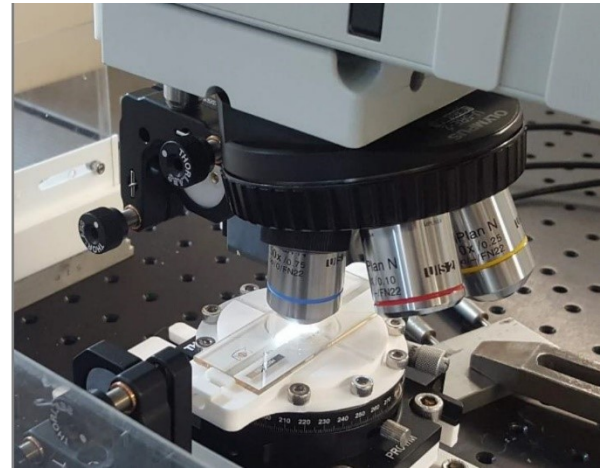
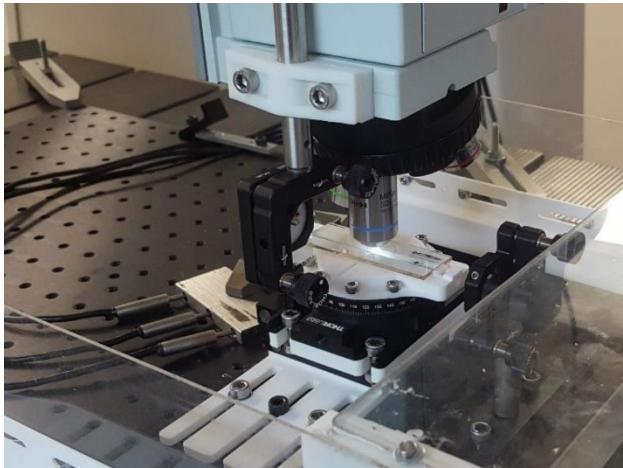
7.13 NMISA

The instrument used was a fully automated, retrofitted SIP5 CMM, using an optical microscope with co-axial illumination. A digital camera was used to capture image frames with a 50x magnification objective. Each frame was analysed to determine the current line mark centre position relative to image centre, with inhouse developed software using the Python programming language. A dual beam plane mirror interferometer is used for the measurement axis.

The SIP5 measurement table moves, while the camera remains stationary. The dual-beam plane mirror laser interferometer measures the table displacement which has movement range of 500 mm. One plane mirror attached as close as possible to the stage micrometer on the measurement table, and the second plane mirror attached the microscope. The measurement table beam axis positioned to be as close as possible to the stage micrometer axis, to reduce Abbe offsets. The face of the stationary mirror is approximately aligned to the centre of the microscope objective (looking from the side). The measurement is therefore taken as the distance between these two plane mirrors to reduce the effect of zero reference point drift. A Perspex "shield" is also placed over the beam path and next to the stage micrometer to reduce air-currents blowing over the beam and thermal gradients.

The stage micrometer is placed on a 3D-printed support, which allows for gentle clamping from the sides (in the direction of measurement). This support is bolted to a rotation stage, allowing for fine alignment of the stage micrometer scale axis to the image axis. Finally, the rotation stage is attached on top of a tilt stage to adjust the vertical alignment using the limited depth-of-field of the 50x magnification (i.e., using the out-of-focus for alignment).





Traceability route

Traceability is through the SIOS dual-beam plane-mirror laser interferometer which was calibrated against a (calibrated) stabilised He-Ne laser.

Principle of line center detection

An image frame is captured by a digital camera. A certain rectangular Region of Interest (ROI) is selected, around the image centre. If required, pre-processing filters can be applied to the ROI. Next, the ROI is divided into horizontal sections and the line centre as well as other line parameters, such as line width, are estimated for each section. The average line centre is calculated as well as the standard deviation. The other parameters can be used to estimate the line quality.

Line centre detection per segment is done by detecting the left and right edge(s) of the visible lines. An average per image column (over Y-axis, where the line scale axis is in the image X-axis) is used to find the edges. Again, certain filters can be applied to this average line, if required. Now, an edge is the interpolated sub-pixel X-axis location where column-average crosses a certain threshold. This threshold can be manually set, or determined as the mid-range value, or the middle of a three-bin histogram.

Normally, the ROI is selected in such a way that only one line mark is inside the ROI. However, the line closest to image X-axis centre is selected if more than one edge pair or line mark are found in the ROI.

Temperature range during measurements

19.50 °C to 20,00 °C

Additional remarks

A linear image calibration factor (e.g., in $\mu\text{m}/\text{pixel}$) is automatically estimated when the measurement starts. This factor relates the image pixels to metre, as measured with the laser interferometer. A correction to the measured position is then applied to subsequent measurements by multiplying the calibration factor with the distance from the linear centre to image X-axis centre. This correction is required since the positioning resolution of X-axis stage is not sufficient to position the current line centre on the image X-axis centre. The X-axis stage position also drifts (in the order of nanometres) immediately after coming to a stop, most likely due to the SIP5 hydrostatic linear bearings.

The correction value is determined for each new frame if a line is found. This value, along with the relative displacement measured by the laser interferometer, thermometer measurements and other variables are continuously logged, when a specific line is measured, and an average result determined over a set time-period. Since the system is completely automated, this can be repeated many times. Furthermore, the software architecture designed to allow for complete recalculation of the result per nominal value per set number. This means that the result and data is not hidden in a “black box” and allows for post-measurement data analysis.

For the reported results, the effect of drift over was reduced by dividing the nominal values into four sub-groups (0 – 250, 250 – 500, 500 – 750 and 750 – 1000), each using the scale zero mark as zero (i.e., 0, 750, 760, ...1000). Each group was repeated 10 times and an average calculated over the 10 sets.